

# Receiver Architectures for MIMO-OFDM Based on a Combined VMP-SP Algorithm

Carles Navarro Manchón, Gunvor E. Kirkelund, Erwin Riegler,  
Lars P. B. Christensen, Bernard H. Fleury.

## Abstract

Iterative information processing, either based on heuristics or analytical frameworks, has been shown to be a very powerful tool for the design of efficient, yet feasible, wireless receiver architectures. Within this context, algorithms performing message-passing on a probabilistic graph, such as the sum-product (SP) and variational message passing (VMP) algorithms, have become increasingly popular.

In this contribution, we apply a combined VMP-SP message-passing technique to the design of receivers for MIMO-OFDM systems. The message-passing equations of the combined scheme can be obtained from the equations of the stationary points of a constrained region-based free energy approximation. When applied to a MIMO-OFDM probabilistic model, we obtain a generic receiver architecture performing iterative channel weight and noise precision estimation, equalization and data decoding. We show that this generic scheme can be particularized to a variety of different receiver structures, ranging from high-performance iterative structures to low complexity receivers. This allows for a flexible design of the signal processing specially tailored for the requirements of each specific application. The numerical assessment of our solutions, based on Monte Carlo simulations, corroborates the high performance of the proposed algorithms and their superiority to heuristic approaches.

## Index Terms

MIMO, OFDM, multi-user detection, message-passing algorithms, belief propagation, mean-field approximation, sum-product, variational message-passing, iterative channel estimation, equalization and data decoding

This work has been submitted to the IEEE for possible publication. Copyright may be transferred without notice, after which this version may no longer be accessible.

## I. INTRODUCTION

During the last two decades, wireless communication systems have undergone a rapid and steep evolution. While old analog systems mainly focused on providing voice communications, today's digital systems offer a plethora of different services such as multimedia communications, web browsing, audio and video streaming, etc. Along with the growing variety of services offered, the amount of users accessing them has also experienced a drastic increase. The combination of applications requiring large amounts of data traffic and high density of users, together with the scarceness of wireless spectrum resources, dictates high spectral efficiency to be an essential target in the design of modern wireless systems.

From a physical layer point of view, the emergence of multiple-input multiple-output (MIMO) techniques [1] together with the development of near-capacity-achieving channel codes, such as turbo [2] or low-density parity check (LDPC) [3] codes, have been the most remarkable steps towards this goal. The use of multiple antennas allows for increasing the theoretical capacity of a wireless channel linearly with the minimum of the number of antenna elements at the transmitter and at the receiver ends [4]. Depending on the specific MIMO technique employed, multiple antennas can be used to exploit the number of degrees of freedom of a wireless channel, its diversity or a mixture of both [5]. The combination with advanced channel codes enables transmission schemes with unprecedented high spectral efficiency. However, in order to realize in practice the performance predicted by theory, advanced receiver architectures combining high performance channel estimators, MIMO detectors and channel decoders are required.

Joint maximum likelihood (ML) receivers are prohibitively complex for most modern communication systems, especially systems with high MIMO order and concatenated codes. A widespread approach for the design of suboptimal, yet efficient receiver architectures is to separate the receiver into several individual blocks, each performing a specific task: channel weight estimation, noise estimation, interference cancellation, equalization or data decoding are some examples. Inspired by the iterative decoding scheme of turbo codes, some structures in which the different constituent blocks exchange information in an iterative manner have been proposed [6]–[10]. In these receivers, each block is designed individually, and the way it exchanges information with the other blocks is based on heuristics. Consequently, while each block is designed to optimally perform its task, the full receiver structure does not necessarily optimize any global

performance criterion. Nevertheless, these structures have shown remarkably good performance at an affordable complexity, while keeping a large degree of flexibility in their design.

Motivated by the success of heuristic iterative approaches, a set of formal frameworks for the design of algorithms performing iterative information processing have arisen in recent years. Among these, methods for variational Bayesian inference in probabilistic models [11] have attracted much attention from the communication research community in recent times. These frameworks allow for the design of iterative algorithms based on the optimization of a global cost function. Typically, they are derived from the stationary points of a discrepancy measure between the probability distribution that needs to be estimated and a postulated auxiliary distribution, the latter distribution providing an estimate of the former. The different frameworks differ on the particular discrepancy measure selected and the restrictions applied to the postulated auxiliary function. We especially highlight two main approaches suggested so far in literature: belief propagation (BP) and mean-field (MF) methods<sup>1</sup>.

BP [16] is a Bayesian inference framework applied to graphical probabilistic models. In its message-passing form –referred to as the sum-product (SP) algorithm [17]– messages are sent from one node of the graphical model to neighboring nodes. The message computation rules for the SP algorithm are obtained from the stationary points of the Bethe free energy [14]. When the graphical model representing the system is free of cycles, the SP algorithm provides exact marginal distributions of the variables in the model. When the graph has cycles, however, the algorithm outputs only an approximation of the marginal distributions and it is, moreover, not guaranteed to converge [18]. In most cases, nonetheless, the obtained marginals are still a high quality approximation of the exact distributions. BP and the SP algorithm have found widespread application in the decoding of channel codes [17], [19], and have also been proposed for the design of iterative receiver structures in wireless communication systems [20]–[24]. However, modifications of the original algorithm are required for parameter estimation problems, such as channel estimation. This has been solved by, e.g., combining the SP algorithm with the expectation-maximization (EM) algorithm [21], [25] or approximating SP messages which are computationally untractable with Gaussian messages [26], [27].

<sup>1</sup>Some authors, e.g. Winn and Bishop [12], [13], consider BP outside the variational Bayesian framework, and usually use the term *variational* only in the context of MF-like approximations. We use, however, the more general view proposed e.g. in [11], [14], [15], which considers BP as another algorithm for variational Bayesian inference.

MF approaches –proposed by Attias in [28] and formulated as the variational Bayesian expectation-maximization (VBEM) principle by Beal [29]– are based on the minimization of the Kullback-Leibler (KL) divergence [30] between a postulated auxiliary function and the distribution to be estimated. The minimization becomes especially computationally tractable under the MF approximation [31], in which the auxiliary function is assumed to completely factorize with respect to the different parameters. The obtained iterative algorithm guarantees convergence in terms of the KL divergence, but convergence to the globally optimum solution can only be guaranteed when the considered problem has a unique single optimum. However, it has proven very useful in the design of iterative receiver structures including channel estimation, e.g., channel estimation and detection for GSM systems [32], iterative multiuser channel estimation, detection and decoding [33] or channel estimation, interference cancellation and detection in OFDM systems [34], [35]. For other applications of MF methods, see [36]–[38]. Message-passing interpretations of this technique on probabilistic graphs have also been proposed in [12], [39], [40] and are commonly referred to as variational message-passing (VMP) techniques.

In this contribution, we apply a hybrid message-passing framework to the design of iterative receivers in a MIMO-OFDM setup. This hybrid framework, recently proposed in [41], [42], combines the SP and VMP algorithms in a unified message-passing technique. Message updates are obtained from the stationary points of a particular region-based free energy approximation [14] of the probabilistic system. Specifically, the combined framework allows for performing VMP in parts of the graph and SP in others, thus enabling a flexible, yet global, design.

From a MIMO-OFDM signal model, we derive a generic message-passing receiver performing channel estimation, MIMO detection and channel decoding in an iterative fashion. Channel estimation is not limited to the estimation of channel weights, but also includes estimation of the noise variance, which proves to be crucial for the operation of the receiver. The application of a unified framework to the whole receiver design unequivocally dictates the type of information that should be exchanged by the individual constituents of the receiver in the form of messages. This is in contrast to heuristic approaches which, for instance, arbitrarily select a-posteriori or extrinsic probabilities to be exchanged between the channel decoder and other modules based on intuitive argumentation or trends observed by simulation results [9], [10].

The generic messages derived can easily be particularized by applying different assumptions and restrictions to the signal model considered. Thus, our framework enables a highly scalable

and flexible design of the signal processing in the receiver. For instance, applying the messages to only part of the factor graph yields simplified architectures performing just a subset of the receiver tasks; also, small modifications to the factor-graph lead to different receiver structures with different performance and computational complexity tradeoffs. These properties are illustrated in our numerical evaluation, where the performance of a few selected instances of our proposed receiver is assessed via Monte Carlo simulations. The presented results demonstrate the high accuracy of our approach, and its superiority to iterative receivers based on heuristics.

The remainder of the paper is organized as follows. The signal model of the MIMO-OFDM system considered is presented in Section II, followed by a brief review of the combined message-passing framework proposed in [41], [42] in Section III. In Section IV, the generic messages to be exchanged in the factor-graph are derived, and the performance of five different receivers obtained from the generic derivation is tested in Section V. Finally, we draw some final conclusions in Section VI.

### A. Notation

Throughout the paper, lower-case boldface letters represent column vectors, while upper-case boldface letters denote matrices;  $(\cdot)^T$  and  $(\cdot)^H$  denote the transpose and conjugate-transpose of a vector or matrix respectively;  $\|\cdot\|$  denotes the Euclidian norm;  $\mathbf{A} \otimes \mathbf{B}$  represents the Kronecker product of matrices  $\mathbf{A}$  and  $\mathbf{B}$ ;  $\mathbf{I}_N$  denotes the identity matrix of dimension  $N$ . Moreover,  $\log$  denotes the natural logarithm;  $f(x) \propto g(x)$  means that  $f(x)$  is equal to  $g(x)$  up to a proportionality constant;  $\langle f(x) \rangle_g$  denotes the expectation of  $f(x)$  over  $g(x)$ , i.e.  $\langle f(x) \rangle_g = \int_x f(x)g(x)dx$ ;  $\mathcal{S} \setminus s$  denotes all elements in the set  $\mathcal{S}$  but  $s$ .

## II. SIGNAL MODEL

In this section a multi-user signal model for MIMO-OFDM is derived. The system is composed by  $M$  synchronous transmitter chains and  $N$  receiver antennas, as depicted in Fig. 1. These transmitters can represent different transmission branches of the same physical transmitter, or physically separated transmitters at different locations. For the  $m$ th transmitter, a finite sequence of information bits  $\mathbf{u}_m$  is encoded, yielding a sequence of coded bits  $\mathbf{c}_m$ . After interleaving, the interleaved coded bits  $\mathbf{c}_m^\pi$  are complex modulated, resulting in the vector  $\mathbf{x}_m^{(d)}$  of complex-modulated data symbols. Finally, the data symbols are multiplexed with the pilot symbols  $\mathbf{x}_m^{(p)}$ ,

giving the transmitted symbols  $\mathbf{x}_m = [x_m(1, 1), \dots, x_m(K, 1), \dots, x_m(1, L), \dots, x_m(K, L)]^T$ , where  $x_m(k, l)$  denotes the symbol sent by the  $m$ th transmitter on the  $k$ th subcarrier of the  $l$ th OFDM symbol of a frame. The transmitted symbols  $\mathbf{x}_m$  are then OFDM modulated using an IFFT and the insertion of a cyclic prefix.

The signal is transmitted through a wide-sense stationary uncorrelated scattering (WSSUS) channel. The channel impulse response from transmitter  $m$  to receiver  $n$  during the transmission of the  $l$ th OFDM symbol  $l$  can be described by

$$g_{nm}(l, \tau) = \sum_{i=1}^{I_{nm}} \alpha_{nm}^{(i)}(l) \delta(\tau - \tau_{nm}^{(i)}) \quad (1)$$

where  $\alpha_{nm}^{(i)}$  and  $\tau_{nm}^{(i)}$  are respectively the complex gain and delay of the  $i^{\text{th}}$  multipath component and  $I_{nm}$  is the number of multipath components. We assume that the channel response is static over the duration of an OFDM symbol, but changes from one OFDM symbol to the next. Also, the maximum delay of each wireless link  $\tau_{nm}^{(I_{nm})}$  is assumed to be smaller than the duration of the OFDM cyclic prefix<sup>2</sup>, so that no inter-symbol interference (ISI) degrades the transmission. From (1), the sample of the channel frequency response at the  $k$ th subcarrier of the  $l$ th OFDM symbol is found to be:

$$h_{nm}(k, l) = \sum_{i=1}^{I_{nm}} \alpha_{nm}^{(i)}(l) e^{-j2\pi k \Delta_f \tau_{nm}^{(i)}}.$$

In this expression,  $\Delta_f$  denotes the OFDM subcarrier spacing.

At the receiver, the signal is OFDM demodulated by discarding the cyclic prefix and applying an FFT on the received samples. Under the previously stated assumptions that the channel is block fading and the maximum delays are smaller than the duration of the cyclic prefix, the signal received at the  $n$ th receive antenna on the  $k$ th subcarrier of the  $l$ th OFDM symbol reads

$$y_n(k, l) = \sum_{m=1}^M h_{nm}(k, l) x_m(k, l) + w_n(k, l), \quad \begin{array}{l} n = 1, \dots, N, \\ k = 1, \dots, K, \\ l = 1, \dots, L, \end{array} \quad (2)$$

with  $w_n(k, l)$  denoting zero-mean additive complex white Gaussian noise (AWGN) with variance  $\lambda^{-1}$ . The equations in (2) can be recast in a matrix-vector notation as

$$\mathbf{y} = \sum_{m=1}^M \mathbf{X}_m \mathbf{h}_m + \mathbf{w} = \sum_{m=1}^M \mathbf{H}_m \mathbf{x}_m + \mathbf{w} \quad (3)$$

<sup>2</sup>We assume without loss of generality that the delays  $\tau_{nm}^{(i)}$  are ordered in increasing order, i.e.  $\tau_{nm}^{(i+1)} \geq \tau_{nm}^{(i)}$ .

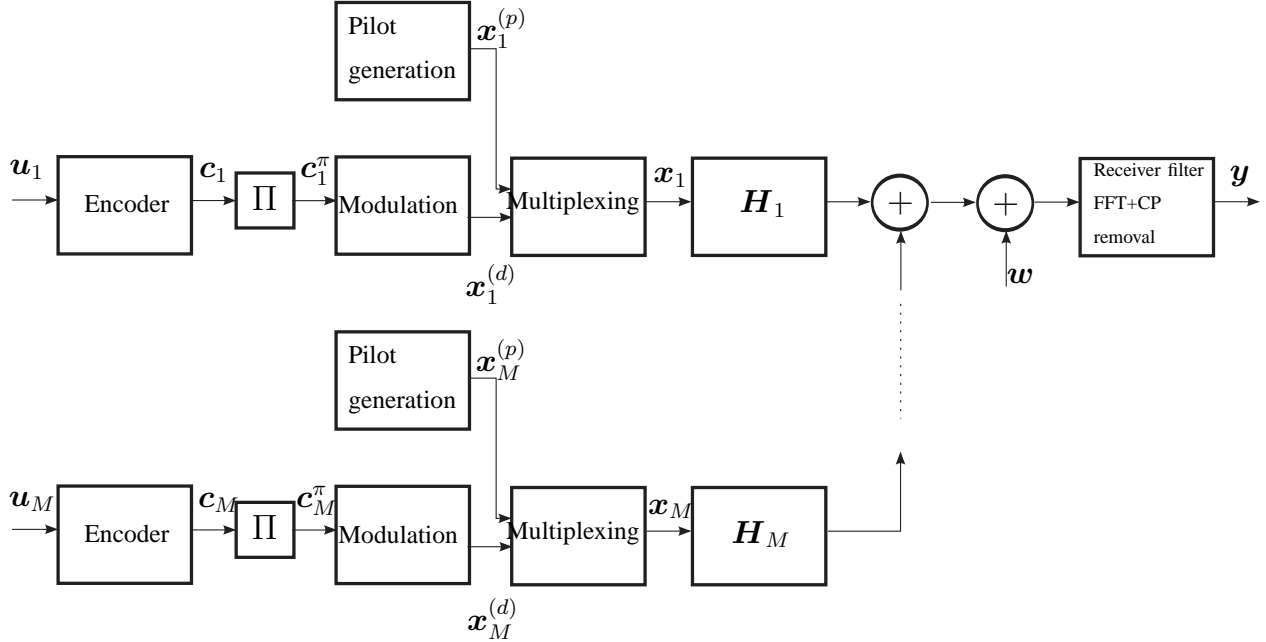


Fig. 1. Block-diagram representation of the transmission model.

where  $\mathbf{y} = [\mathbf{y}_1^T, \dots, \mathbf{y}_N^T]^T$ , with  $\mathbf{y}_n = [y_n(1, 1), \dots, y_n(K, 1), \dots, y_n(1, L), \dots, y_n(K, L)]^T$  denoting the received signal at the  $n$ th receive antenna for a frame of  $K$  subcarriers and  $L$  OFDM symbols. Additionally,  $\mathbf{h}_m = [\mathbf{h}_{1m}^T, \dots, \mathbf{h}_{Nm}^T]^T$ ,  $\mathbf{X}_m = \mathbf{I}_N \otimes \text{diag}\{\mathbf{x}_m\}$ ,  $\mathbf{H}_m = [\text{diag}\{\mathbf{h}_{1m}\}, \dots, \text{diag}\{\mathbf{h}_{Nm}\}]^T$  and  $\mathbf{h}_{nm} = [h_{nm}(1, 1), \dots, h_{nm}(K, 1), \dots, h_{nm}(1, L), \dots, h_{nm}(K, L)]^T$ . Equation (3) can be further compressed as

$$\mathbf{y} = \mathbf{X}\mathbf{h} + \mathbf{w} = \mathbf{H}\mathbf{x} + \mathbf{w}$$

where  $\mathbf{x} = [\mathbf{x}_1^T, \dots, \mathbf{x}_M^T]^T$ ,  $\mathbf{h} = [\mathbf{h}_1^T, \dots, \mathbf{h}_M^T]^T$ ,  $\mathbf{X} = [\mathbf{X}_1, \dots, \mathbf{X}_M]$  and  $\mathbf{H} = [\mathbf{H}_1, \dots, \mathbf{H}_M]$ .

### III. MESSAGE PASSING TECHNIQUES

In this section, we briefly introduce message-passing techniques on factor graphs. First, we define the concept of factor graph on a probabilistic model, followed by the description of two standard message-passing schemes: the sum-product (SP) algorithm [17] and the variational message-passing (VMP) algorithm [12]. Finally, we show how to combine both algorithms to perform hybrid VMP and SP message passing in a factor graph [41].

### A. Factor Graphs for Probabilistic Models

Let  $p(\mathbf{z})$  be the probability density function (pdf) of a vector  $\mathbf{z}$  of random variables  $z_i$  ( $i \in \mathcal{I}$ ) which factorizes according to

$$p(\mathbf{z}) = \frac{1}{Z} \prod_{a \in \mathcal{A}} f_a(\mathbf{z}_a) \quad (4)$$

where  $\mathbf{z}_a = (z_i | i \in \mathcal{N}(a))^T$  with  $\mathcal{N}(a) \subseteq \mathcal{I}$  for all  $a \in \mathcal{A}$  and  $Z = \int_{\mathbf{z}} \prod_{a \in \mathcal{A}} f_a(\mathbf{z}_a) d\mathbf{z}$  is a normalization constant. We also define  $\mathcal{N}(i) \triangleq \{a \in \mathcal{A} | i \in \mathcal{N}(a)\}$  for all  $i \in \mathcal{I}$ . Similarly,  $\mathcal{N}(a) = \{i \in \mathcal{I} | a \in \mathcal{N}(i)\}$  for all  $a \in \mathcal{A}$ . The above factorization can be graphically represented by means of a factor graph [17]. A factor graph<sup>3</sup> is a bipartite graph having a variable node  $i$  (typically represented by a circle) for each variable  $z_i$ ,  $i \in \mathcal{I}$  and a factor node  $a$  (represented by a square) for each factor  $f_a$ ,  $a \in \mathcal{A}$ . An edge connects a variable node  $i$  to a factor node  $a$  if, and only if, the variable  $z_i$  is an argument of the factor function  $f_a$ . The set  $\mathcal{N}(i)$  contains all factor nodes connected to a variable node  $i \in \mathcal{I}$  and  $\mathcal{N}(a)$  is the set of all variable nodes connected to a factor node  $a \in \mathcal{A}$ .

Factor graphs provide a compact and intuitive representation of the statistical dependencies among the random variables in a probabilistic model. Furthermore, they enable the design of a class of iterative signal processing algorithms which are based on the nodes of the graph iteratively exchanging information (messages) with their neighbors (connected nodes). This class of algorithms has been coined *message-passing* techniques, and in the following we will describe the two instances of these techniques which have been most widely applied to signal processing for communication systems: the SP and VMP algorithms.

### B. The Sum-Product Algorithm

The SP algorithm is a message-passing algorithm that computes the exact marginal distributions  $p_i(z_i)$  of the variables  $z_i$  associated to the joint distribution  $p(\mathbf{z})$  for tree-shaped factor graphs. When the factor graph does not have a tree structure, the outcome of the algorithm is only an approximation of the true marginal, and the approximate marginals  $b_i(z_i) \approx p_i(z_i)$  are called beliefs. The message-passing algorithm is derived from the equations of the stationary points of the constrained Bethe free energy [14].

<sup>3</sup>We will use Tanner factor graphs [17] throughout this article

The algorithm operates iteratively by exchanging messages from variable nodes to factor nodes and vice-versa. The message computation rules for the SP algorithm read

$$m_{a \rightarrow i}(z_i) = d_a \langle f_a(\mathbf{z}_a) \rangle_{\prod_{j \in \mathcal{N}(a) \setminus i} n_{j \rightarrow a}}, \quad \forall a \in \mathcal{A}, i \in \mathcal{N}(a)$$

$$n_{i \rightarrow a}(z_i) = \prod_{c \in \mathcal{N}(i) \setminus a} m_{c \rightarrow i}(z_i), \quad \forall i \in \mathcal{I}, a \in \mathcal{N}(i)$$

where  $d_a$  ( $a \in \mathcal{A}$ ) are positive constants ensuring that the beliefs are normalized to one. Often the constants  $d_a$  need not be calculated explicitly, and it is enough to normalize the beliefs after convergence of the algorithm (see [42] for more details on normalization issues). We use the notation  $n_{(\cdot) \rightarrow (\cdot)}$  for output messages from a variable node to a factor node and  $m_{(\cdot) \rightarrow (\cdot)}$  for input messages from a factor node to a variable node. This convention will be kept through the rest of the paper, also for other message-passing schemes.

The variables' beliefs can be calculated at any point during the iterative algorithm as

$$b_i(z_i) = \prod_{a \in \mathcal{N}(i)} m_{a \rightarrow i}(z_i) \quad \forall i \in \mathcal{I}.$$

The SP algorithm acquired great popularity through its application to iterative decoding of, among others, turbo codes and LDPC codes, and has since then been used for the design of many iterative algorithms in a wide variety of fields [21].

### C. The Variational Message-Passing Algorithm

The VMP algorithm is an alternative message-passing technique which is derived based on the minimization of the variational free energy subject to the mean-field approximation constraint on the beliefs. While it does not guarantee the computation of exact marginals (even for tree-shaped graphs), its convergence is guaranteed by ensuring that the variational free energy of the computed beliefs is non-increasing at each step of the algorithm [14].

The operation of the VMP algorithm is analogous to the SP algorithm; the message computation rules read

$$m_{a \rightarrow i}(z_i) = \exp\langle \log f_a(\mathbf{z}_a) \rangle_{\prod_{j \in \mathcal{N}(a) \setminus i} n_{j \rightarrow a}}, \quad \forall a \in \mathcal{A}, i \in \mathcal{N}(a) \quad (5)$$

$$n_{i \rightarrow a}(z_i) = e_i \prod_{c \in \mathcal{N}(i) \setminus a} m_{c \rightarrow i}(z_i) \quad \forall i \in \mathcal{I}, a \in \mathcal{N}(i) \quad (6)$$

where  $e_i$  ( $i \in \mathcal{I}$ ) are positive constants ensuring that  $n_{i \rightarrow a}$  are normalized. As in the SP algorithm, the beliefs can be obtained as

$$b_i(z_i) = e_i \prod_{c \in \mathcal{N}(i)} m_{c \rightarrow i}(z_i) = n_{i \rightarrow a}(z_i) \quad \forall i \in \mathcal{I}, a \in \mathcal{N}(i).$$

The VMP algorithm has recently attracted the attention of the wireless communication research community due to its suitability for conjugate-exponential probabilistic models [12]. The computation rule for input messages from factor to variable nodes allows for the obtention of closed-form expressions in many cases in which the SP algorithm typically requires some type of numerical approximation.

It is shown in [42] that a message-passing interpretation of the EM algorithm can be obtained from the VMP algorithm. Assume that for a certain subset of variables  $z_i$ ,  $i \in \mathcal{E} \subseteq \mathcal{I}$  we want to apply an EM update while still using VMP for the rest of variables. To do so, the beliefs  $b_i$  are restricted to fulfill the constraint  $b_i(z_i) = \delta(z_i - \tilde{z}_i)$  for all  $i \in \mathcal{E}$  additionally to the mean-field factorization and normalization constraints. Minimizing the variational free energy subject to these conditions leads to a message passing algorithm identical to the one described in (5) and (6) except that the messages  $n_{i \rightarrow a}$  for all  $i \in \mathcal{E}$  and  $a \in \mathcal{N}(i)$  are replaced by

$$n_{i \rightarrow a}(z_i) = \delta(z_i - \tilde{z}_i) \quad \text{with} \quad \tilde{z}_i = \operatorname{argmax}_{z_i} \left( \prod_{a \in \mathcal{N}(i)} m_{a \rightarrow i}(z_i) \right). \quad (7)$$

#### D. Combined VMP-SP Algorithm

As stated previously in this section, the VMP and the SP algorithms are two message-passing techniques suitable for different types of models. While SP is especially suitable in models with deterministic factor nodes, e.g. code or modulation constraints, VMP has the advantage of yielding closed-form computationally tractable expressions in conjugate-exponential models, as are found in channel weight estimation and noise variance estimation problems. Based on these facts, it seems natural to try to combine the two methods in a unified scheme capable of preserving the advantages of both.

A combined message-passing scheme based on the SP and VMP algorithms was recently proposed in [41], [42]. This hybrid technique is based on splitting the factor graph into two different parts: a VMP part and a SP part. To do this, part of the factor nodes are assigned to

the VMP set ( $\mathcal{A}_{\text{VMP}}$ ) and the rest are assigned to the SP set ( $\mathcal{A}_{\text{SP}}$ ). Given this classification, we can express the probabilistic model in (4) as

$$p(\mathbf{z}) = \frac{1}{Z} \overbrace{\prod_{a \in \mathcal{A}_{\text{VMP}}} f_a(\mathbf{z}_a)}^{\text{VMPpart}} \overbrace{\prod_{c \in \mathcal{A}_{\text{SP}}} f_c(\mathbf{z}_c)}^{\text{SPpart}}$$

where  $\mathcal{A}_{\text{VMP}} \cup \mathcal{A}_{\text{SP}} = \mathcal{A}$  and  $\mathcal{A}_{\text{VMP}} \cap \mathcal{A}_{\text{SP}} = \emptyset$ . By applying the Bethe approximation to the SP part and the mean-field approximation on the VMP part, a new message-passing scheme is derived from the stationary points of the region-based free energy [41], [42]. The message computation rules for this algorithm read

$$m_{a \rightarrow i}^{\text{VMP}}(z_i) = \exp(\log f_a(\mathbf{z}_a)) \prod_{j \in \mathcal{N}(a) \setminus i} n_{j \rightarrow a}, \quad \forall a \in \mathcal{A}_{\text{VMP}}, i \in \mathcal{N}(a) \quad (8)$$

$$m_{a \rightarrow i}^{\text{SP}}(z_i) = d_a \langle f_a(\mathbf{z}_a) \rangle \prod_{j \in \mathcal{N}(a) \setminus i} n_{j \rightarrow a}, \quad \forall a \in \mathcal{A}_{\text{SP}}, i \in \mathcal{N}(a) \quad (9)$$

$$n_{i \rightarrow a}(z_i) = e_i \prod_{c \in \mathcal{N}(i) \cap \mathcal{A}_{\text{VMP}}} m_{c \rightarrow i}^{\text{VMP}}(z_i) \prod_{c \in \mathcal{N}(i) \cap \mathcal{A}_{\text{SP}} \setminus a} m_{c \rightarrow i}^{\text{SP}}(z_i) \quad \forall i \in \mathcal{I}, a \in \mathcal{N}(i) \quad (10)$$

where, again,  $d_a$  and  $e_i$  are positive constants ensuring normalized beliefs. The computation rules for messages outgoing factor nodes are preserved: for factor nodes in the VMP part ( $a \in \mathcal{A}_{\text{VMP}}$ ) the messages are computed using (8) as in standard VMP; for factor nodes in the SP part ( $a \in \mathcal{A}_{\text{SP}}$ ) the messages are computed via (9), which corresponds to a standard SP message. A message from a variable node  $i$  to a factor node  $a$  is computed as a VMP message when  $a \in \mathcal{A}_{\text{VMP}}$  and as a SP message when  $a \in \mathcal{A}_{\text{SP}}$ , as can be deduced from (10).

As with the VMP and SP algorithms, the beliefs of the variables can be retrieved at any stage of the algorithm as

$$b_i(z_i) = e_i \prod_{a \in \mathcal{N}(i) \cap \mathcal{A}_{\text{VMP}}} m_{a \rightarrow i}^{\text{VMP}}(z_i) \prod_{a \in \mathcal{N}(i) \cap \mathcal{A}_{\text{SP}}} m_{a \rightarrow i}^{\text{SP}}(z_i) \quad \forall i \in \mathcal{I}.$$

Note that we can apply the EM restriction to the belief of variables  $z_i$  which are only connected to VMP factors (i.e.  $\mathcal{N}(i) \cap \mathcal{A}_{\text{SP}} = \emptyset$ ). In that case, the message update rules remain the same except that the message  $n_{i \rightarrow a}$  in (10) is replaced by (7) for the selected variables.

#### IV. MIMO-OFDM RECEIVER BASED ON COMBINED VMP-SPA

In this section, we present a generic iterative receiver for MIMO-OFDM systems based on the mixed VMP and SP message-passing strategy outlined in Section III-D. Recalling the signal model presented in Section II, we can now postulate the probabilistic model to which we will

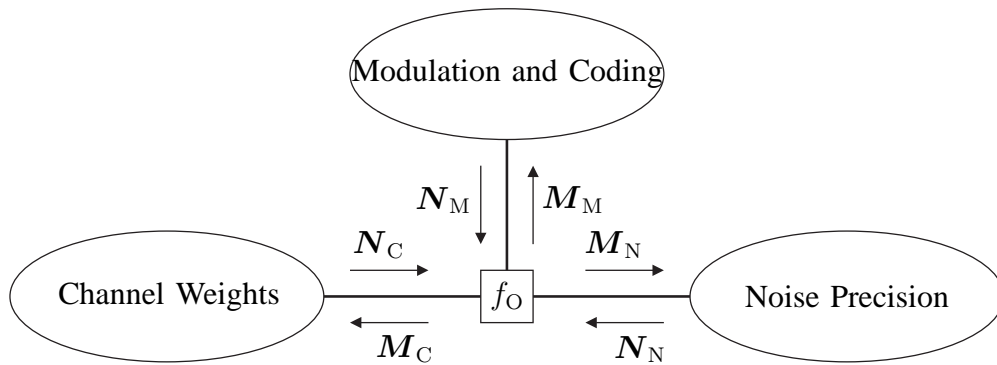


Fig. 2. Generic factor graph of the receiver.

apply the combined VMP-SP technique. In our case, we identify the observation to be the received signal vector  $\mathbf{y}$ . As unknown parameters, we include the vector of information bits  $\mathbf{u} = [\mathbf{u}_1^T, \dots, \mathbf{u}_M^T]^T$ , the vector of coded bits  $\mathbf{c} = [\mathbf{c}_1^T, \dots, \mathbf{c}_M^T]^T$ , the vector of modulated symbols  $\mathbf{x} = [\mathbf{x}_1, \dots, \mathbf{x}_M]^T$ , the vector of complex channel weights  $\mathbf{h} = [\mathbf{h}_1, \dots, \mathbf{h}_M]^T$  and the AWGN precision  $\lambda$ . The system function of our model is the joint pdf of all parameters, which can be factorized as

$$p(\mathbf{u}, \mathbf{c}, \mathbf{x}, \mathbf{h}, \lambda, \mathbf{y}) = \underbrace{p(\mathbf{y}|\mathbf{h}, \mathbf{x}, \lambda)}_{f_O} \underbrace{p(\mathbf{h})}_{f_C} \underbrace{p(\lambda)}_{f_N} \underbrace{p(\mathbf{x}, \mathbf{c}, \mathbf{u})}_{f_M} \quad (11)$$

where we have chosen to group the factors on the right-hand side into four functions. Factor  $f_O(\mathbf{y}, \mathbf{h}, \mathbf{x}, \lambda) \triangleq p(\mathbf{y}|\mathbf{h}, \mathbf{x}, \lambda)$  denotes the likelihood of the channel weights  $\mathbf{h}$ , the noise precision  $\lambda$  and the transmitted symbols  $\mathbf{x}$  given the observation  $\mathbf{y}$ . Factor  $f_C(\mathbf{h}) \triangleq p(\mathbf{h})$  contains the assumed prior model of the channel weights, which is relevant for channel weight estimation. Function  $f_N(\lambda) \triangleq p(\lambda)$ , likewise, contains the assumed prior model for the noise precision parameter  $\lambda$  which defines how estimation of the noise precision is done. Finally, function  $f_M(\mathbf{x}, \mathbf{c}, \mathbf{u}) \triangleq p(\mathbf{x}, \mathbf{c}, \mathbf{u})$  denotes the modulation and code constraints. Note that further factorization of the factors in (11) is possible and will, in fact, be used later in this section.

A schematic factor-graph-like representation of the model in (11) is depicted in Fig. 2. The observation factor node  $f_O$  is connected to three ovals: channel weights, noise precision and modulation and coding. Each of the ovals represents a subgraph corresponding to factors  $f_C$ ,  $f_N$  and  $f_M$  in (11). The three subgraphs are connected to  $f_O$ , which reads

$$f_O(\mathbf{y}, \mathbf{x}, \mathbf{h}, \lambda) \propto \lambda^{KNL} \exp \{-\lambda \|\mathbf{y} - \mathbf{X}\mathbf{h}\|^2\} = \lambda^{KNL} \exp \{-\lambda \|\mathbf{y} - \mathbf{H}\mathbf{x}\|^2\}.$$

Each of the subgraphs in Fig. 2 will be detailed in the remainder of this section. For now, we define the sets  $\mathcal{A}_C$ ,  $\mathcal{A}_N$  and  $\mathcal{A}_M$  as the set of factor nodes inside the channel weights, noise precision and modulation and coding subgraphs respectively. Likewise, we define the sets  $\mathcal{I}_C$ ,  $\mathcal{I}_N$  and  $\mathcal{I}_M$  as the set of variable nodes inside the channel weights, noise precision and modulation and coding subgraphs respectively. With these definitions, the set of all factor nodes in the graph is given by<sup>4</sup>

$$\mathcal{A} = \{f_O\} \cup \mathcal{A}_C \cup \mathcal{A}_N \cup \mathcal{A}_M,$$

and the set of all variable nodes reads

$$\mathcal{I} = \mathcal{I}_C \cup \mathcal{I}_N \cup \mathcal{I}_M.$$

From the observation factor node  $f_O$ , sets of messages  $M_C$ ,  $M_N$  and  $M_M$  are sent to the respective subgraphs. These sets are composed of individual messages  $m_{f_O \rightarrow z}$ ,  $z \in \mathcal{I}$ . The specific composition of the sets of messages depends on the exact configuration of variable and factor nodes of the corresponding subgraph, which will be described later in the section. After processing is completed at each subgraph, sets of messages  $N_C$ ,  $N_N$  and  $N_M$ , which correspond to the updated estimates of the channel weights, the noise precision and the transmitted symbols respectively, are send back to  $f_O$ .

In order to apply the combined VMP-SP algorithm, we need to define which factor nodes are assigned to the VMP set  $\mathcal{A}_{\text{VMP}}$  and which are assigned to the SP set  $\mathcal{A}_{\text{SP}}$ . We select the following splitting:

$$\begin{aligned} \mathcal{A}_{\text{VMP}} &\triangleq \{f_O\} \cup \mathcal{A}_C \cup \mathcal{A}_N \\ \mathcal{A}_{\text{SP}} &\triangleq \mathcal{A}_M \end{aligned}$$

i.e. the observation factor node and all factors in the channel weight and noise precision subgraphs are assigned to the VMP set, and all factor nodes in the modulation and coding subgraph are assigned to the SP set.

In the remainder of this section, we will present the details of each of the subgraphs, with several alternative factor-graph representations yielding different message-passing configurations.

<sup>4</sup>With a slight abuse of notation, from this point on we use the names of functions and variables as indices of the sets  $\mathcal{A}$  and  $\mathcal{I}$  respectively.

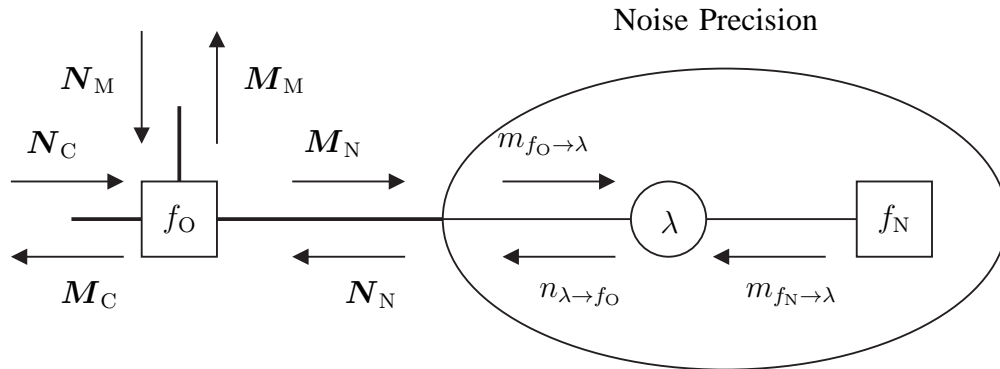


Fig. 3. Subgraph corresponding to the noise precision prior model.

The performance of the individual receiver structures obtained will be evaluated and compared in Section V.

#### A. Noise Precision Subgraph

The noise precision subgraph is the graphical representation of  $f_N$  in (11), which we specify now as

$$f_N(\lambda) \triangleq p(\lambda)$$

where  $p(\lambda)$  denotes the prior distribution of  $\lambda$ . With this, we can now specify the sets

$$\mathcal{A}_N = \{f_N\}$$

$$\mathcal{I}_N = \{\lambda\}.$$

The factor graph representation of the subgraph is depicted in Fig. 3. It only consists of the variable node  $\lambda$  and the factor node  $f_N$ . Since there is only one variable node connected to  $f_O$ , the set of messages  $\mathbf{M}_N$  reduces to  $\mathbf{M}_N = \{m_{f_O \rightarrow \lambda}\}$ . Analogously,  $\mathbf{N}_N = \{n_{\lambda \rightarrow f_O}\}$ .

According to the message-computation rules given in Section III, the message transmitted from  $f_O$  to  $\lambda$  is calculated as

$$m_{f_O \rightarrow \lambda}(\lambda) = \exp \{ \langle \log f_O(\mathbf{y}, \mathbf{x}, \mathbf{h}, \lambda) \rangle_{N_C N_M} \} = \lambda^{KLN} \exp \{ -\lambda A \} \quad (12)$$

with

$$A = \|\mathbf{y} - \hat{\mathbf{X}}\hat{\mathbf{h}}\|^2 + \text{Tr} \left\{ \hat{\mathbf{B}}^H \hat{\mathbf{C}} \hat{\mathbf{B}} + \hat{\mathbf{B}}^H \hat{\mathbf{H}}^H \hat{\mathbf{H}} \hat{\mathbf{B}} \right\} + \text{Tr} \left\{ \hat{\mathbf{X}} \hat{\Sigma}_h \hat{\mathbf{X}}^H \right\}.$$

In the above expression,  $\hat{\mathbf{h}} = \langle \mathbf{h} \rangle_{N_C}$ ,  $\hat{\mathbf{H}} = \langle \mathbf{H} \rangle_{N_C}$ ,  $\hat{\mathbf{x}} = \langle \mathbf{x} \rangle_{N_M}$ ,  $\hat{\mathbf{X}} = \langle \mathbf{X} \rangle_{N_M}$  are the means of  $\mathbf{h}$ ,  $\mathbf{H}$ ,  $\mathbf{x}$  and  $\mathbf{X}$  respectively taken with respect to the channel weights and modulation and coding output messages. Moreover,  $\hat{\Sigma}_{\mathbf{h}} = \langle \mathbf{h}\mathbf{h}^H \rangle_{N_C} - \hat{\mathbf{h}}\hat{\mathbf{h}}^H$ , and  $\hat{\mathbf{C}} = \langle \mathbf{H}^H\mathbf{H} \rangle_{N_M} - \hat{\mathbf{H}}^H\hat{\mathbf{H}}$ . Finally,  $\hat{\mathbf{B}} = \mathbf{U}\mathbf{\Lambda}^{1/2}$  where  $\mathbf{\Lambda}$  is the diagonal matrix of eigenvalues and  $\mathbf{U}$  is the matrix containing the eigenvectors of  $\hat{\Sigma}_{\mathbf{x}} = \langle \mathbf{x}\mathbf{x}^H \rangle_{N_M} - \hat{\mathbf{x}}\hat{\mathbf{x}}^H$ , i.e.  $\hat{\Sigma}_{\mathbf{x}} = \mathbf{U}\mathbf{\Lambda}\mathbf{U}^H$ .

The message in (12) is proportional to the pdf of a complex central Wishart distribution of dimension 1,  $KLN + 1$  degrees of freedom and associated covariance  $A^{-1}$  [43]. We select the prior pdf  $p(\lambda)$  to be conjugate, i.e., a complex Wishart. This yields the message

$$m_{f_N \rightarrow \lambda}(\lambda) = p(\lambda) \propto \lambda^{a-1} \exp\{-\lambda A_{\text{prior}}\}.$$

Given the two incoming messages  $m_{f_N \rightarrow \lambda}$  and  $m_{f_O \rightarrow \lambda}$ , the outgoing message from  $\lambda$  is also proportional to a complex Wishart pdf

$$n_{\lambda \rightarrow f_O}(\lambda) \propto m_{f_N \rightarrow \lambda}(\lambda)m_{f_O \rightarrow \lambda}(\lambda) \propto \lambda^{KLN+a-1} \exp\{-\lambda(A + A_{\text{prior}})\}.$$

Since usually no prior information on the noise precision is available at the receiver, we select  $p(\lambda)$  non-informative with parameters  $a = 0$  and  $A_{\text{prior}} = 0$ . With this choice, the mean of  $\lambda$  with respect to  $N_N$  reads

$$\hat{\lambda} = \langle \lambda \rangle_{N_N} = \frac{KLN}{A}. \quad (13)$$

Note that the above update for  $\hat{\lambda}$  coincides with the ML estimate of the noise precision. Since, as we will see later in the section, only the first moment of  $\lambda$  is needed to compute other messages, it is sufficient to pass just this value to the rest of the graph.

### B. Channel Weights Subgraph

The channel weights subgraph includes the graphical description of the factor  $f_C$  in (11). We will present in the following two alternative subgraphs representing two possible definitions of  $f_C$ : in the first one, coined *joint* channel weights subgraph, all channel weights for all transmit antennas are grouped together in a single variable node  $\mathbf{h}$ ; in the second one, which we refer to as *disjoint* channel weights subgraph, the weights are split into  $M$  variable nodes  $\mathbf{h}_1, \dots, \mathbf{h}_M$  each of them containing the channel weights associated with an individual transmit antenna.

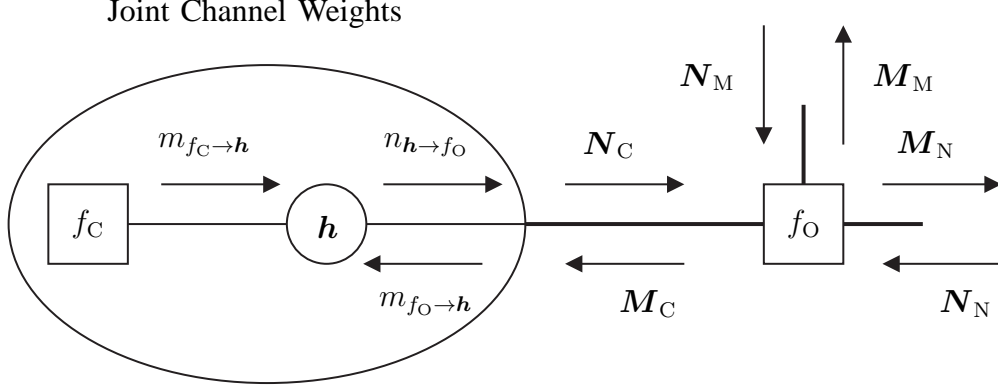


Fig. 4. Subgraph corresponding to the prior model of the joint channel weights.

1) *Joint Channel Weights Model*: The joint channel weights subgraph is obtained from the following definition:

$$f_C(\mathbf{h}) \triangleq p(\mathbf{h})$$

with  $p(\mathbf{h})$  denoting the prior pdf of the vector of channel weights  $\mathbf{h}$ . Using this model for  $f_C$  leads to defining the factor and variable node sets as

$$\mathcal{A}_C = \{f_C\}$$

$$\mathcal{I}_C = \{\mathbf{h}\}.$$

The factor graph describing the joint channel weight option is presented in Fig. 4. As there is only one variable node connected to the factor node  $f_O$ , the set of input messages to the channel weights subgraph is simply  $\mathcal{M}_C = \{m_{f_O \rightarrow \mathbf{h}}\}$  and the set of output messages is the singleton  $\mathcal{N}_C = \{n_{\mathbf{h} \rightarrow f_O}\}$ .

The message from  $f_O$  to  $\mathbf{h}$  is given by

$$m_{f_O \rightarrow \mathbf{h}}(\mathbf{h}) = \exp\{\langle \log f_O(\mathbf{y}, \mathbf{x}, \mathbf{h}, \lambda) \rangle_{N_M N_N}\} \propto \exp\left\{-\hat{\lambda} \left(\|\mathbf{y} - \hat{\mathbf{X}}\mathbf{h}\|^2 + \mathbf{h}^H \hat{\mathbf{D}}\mathbf{h}\right)\right\}$$

with  $\hat{\mathbf{D}} = \langle \mathbf{X}^H \mathbf{X} \rangle_{N_M} - \hat{\mathbf{X}}^H \hat{\mathbf{X}}$ . Hence,  $m_{f_O \rightarrow \mathbf{h}}(\mathbf{h})$  is proportional to a Gaussian pdf. We also impose the prior  $p(\mathbf{h})$  to be Gaussian, which yields the message

$$m_{f_C \rightarrow \mathbf{h}}(\mathbf{h}) = p(\mathbf{h}) \propto \exp\left\{-\left(\mathbf{h} - \mathbf{h}_{\text{prior}}\right)^H \Sigma_{\mathbf{h}_{\text{prior}}}^{-1} \left(\mathbf{h} - \mathbf{h}_{\text{prior}}\right)\right\}.$$

For most practical channels it is reasonable to assume that  $\mathbf{h}_{\text{prior}} = 0$ . The receiver needs an estimate of the prior covariance of the channel  $\Sigma_{\mathbf{h}_{\text{prior}}}$ . In order to obtain the outgoing message

$n_{\mathbf{h} \rightarrow f_{\text{O}}}(\mathbf{h})$ , the two incoming messages are combined, leading to

$$n_{\mathbf{h} \rightarrow f_{\text{O}}}(\mathbf{h}) \propto m_{f_{\text{O}} \rightarrow \mathbf{h}}(\mathbf{h}) m_{f_{\text{C}} \rightarrow \mathbf{h}}(\mathbf{h}) \propto \exp \left\{ -(\mathbf{h} - \hat{\mathbf{h}})^{\text{H}} \hat{\Sigma}_{\mathbf{h}}^{-1} (\mathbf{h} - \hat{\mathbf{h}}) \right\}$$

Thus,  $n_{\mathbf{h} \rightarrow f_{\text{O}}}$  is proportional to a Gaussian pdf with covariance matrix

$$\hat{\Sigma}_{\mathbf{h}} = \left( \hat{\lambda} \hat{\mathbf{X}}^{\text{H}} \hat{\mathbf{X}} + \hat{\lambda} \hat{\mathbf{D}} + \Sigma_{\mathbf{h}_{\text{prior}}}^{-1} \right)^{-1}$$

and mean value

$$\hat{\mathbf{h}} = \hat{\Sigma}_{\mathbf{h}} \left( \hat{\lambda} \hat{\mathbf{X}}^{\text{H}} \mathbf{y} + \Sigma_{\mathbf{h}_{\text{prior}}}^{-1} \mathbf{h}_{\text{prior}} \right).$$

2) *Disjoint Channel Weights Model*: The disjoint channel weights subgraph is obtained by factorizing  $f_{\text{C}}$  with respect to each transmitter. More specifically, we define

$$f_{\text{C}}(\mathbf{h}) = \prod_{m=1}^M f_{\text{C}_m}(\mathbf{h}_m)$$

with  $f_{\text{C}_m}(\mathbf{h}_m) \triangleq p(\mathbf{h}_m)$ ,  $m = 1, \dots, M$  denoting the prior pdf of the channel weights for the  $m$ th transmit antenna. We also specify the sets

$$\mathcal{A}_{\text{C}} = \{f_{\text{C}_m} | m = 1, \dots, M\}$$

$$\mathcal{I}_{\text{C}} = \{\mathbf{h}_m | m = 1, \dots, M\}.$$

Fig. 5 shows the factor graph of the disjoint channel weights model with the above definitions. With this configuration, the channel weight vector  $\mathbf{h}$  is split into  $M$  variable nodes  $\mathbf{h}_1, \dots, \mathbf{h}_M$ , each of them containing the weights associated with one transmit antenna. Each of these variable nodes is furthermore connected to a factor node  $f_{\text{C}_m}$ . Due to this separation, the set of incoming messages reads  $\mathcal{M}_{\text{C}} = \{m_{f_{\text{O}} \rightarrow \mathbf{h}_m} | m = 1, \dots, M\}$ , while the set of outgoing messages is  $\mathcal{N}_{\text{C}} = \{n_{\mathbf{h}_m \rightarrow f_{\text{O}}} | m = 1, \dots, M\}$ . With this structure, the channel weight vectors are estimated sequentially by iterating through the transmit antenna index  $m$ .

For the  $m$ th transmit antenna, the incoming message reads

$$\begin{aligned} m_{f_{\text{O}} \rightarrow \mathbf{h}_m}(\mathbf{h}_m) &= \exp \left\{ \langle \log f_{\text{O}}(\mathbf{y}, \mathbf{x}, \mathbf{h}, \lambda) \rangle_{\mathcal{N}_{\text{M}} \mathcal{N}_{\text{N}} \mathcal{N}_{\text{C}}^{(m)}} \right\} \\ &\propto \exp \left\{ -\hat{\lambda} \left( \left\| \mathbf{y} - \sum_{m' \neq m} \hat{\mathbf{X}}_{m'} \hat{\mathbf{h}}_{m'} - \hat{\mathbf{X}}_m \mathbf{h}_m \right\|^2 + \mathbf{h}_m^{\text{H}} \hat{\mathbf{D}}_m \mathbf{h}_m \right) \right\} \end{aligned}$$

where  $\mathcal{N}_{\text{C}}^{(m)} = \{n_{\mathbf{h}_{m'} \rightarrow f_{\text{O}}} | \forall m' = 1, \dots, M, m' \neq m\}$  denotes the set of all output channel weight messages except the  $m$ th one. Furthermore,  $\hat{\mathbf{h}}_{m'} = \langle \mathbf{h}_{m'} \rangle_{\mathcal{N}_{\text{C}}^{(m)}}$ ,  $\hat{\mathbf{X}}_m = \langle \mathbf{X}_m \rangle_{\mathcal{N}_{\text{M}}}$  and  $\hat{\mathbf{D}}_m = \langle \mathbf{X}_m^{\text{H}} \mathbf{X}_m \rangle_{\mathcal{N}_{\text{M}}}$ .

## Disjoint Channel Weights

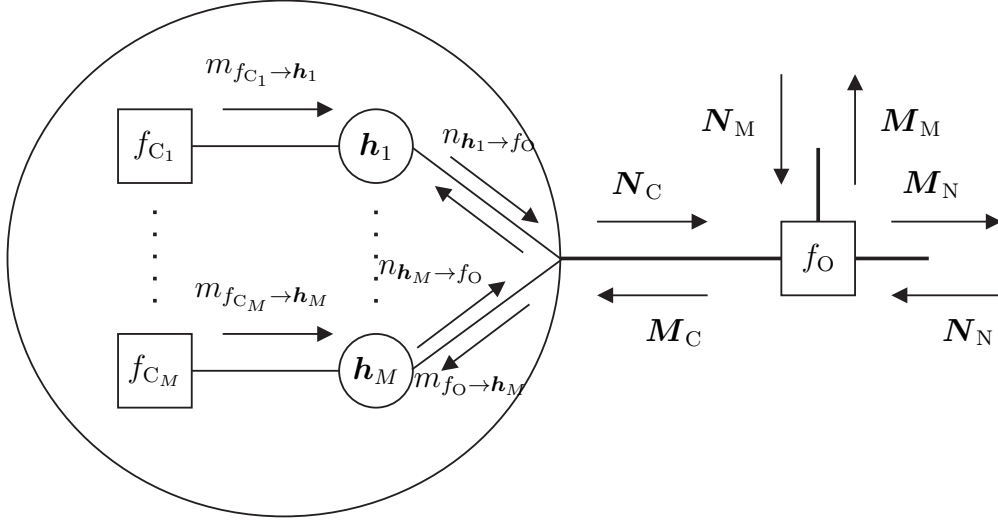


Fig. 5. Subgraph corresponding to the prior model of the disjoint channel weights.

$\hat{\mathbf{X}}_m^H \hat{\mathbf{X}}_m$ . Again,  $m_{f_O \rightarrow h_m}$  is observed to be proportional to a Gaussian pdf. Analogously to the joint channel weights case, we need to specify the prior of each individual channel vector  $\mathbf{h}_m$ . Defining them as Gaussians leads to the message

$$m_{f_{C_m} \rightarrow h_m}(\mathbf{h}_m) = p(\mathbf{h}_m) \propto \exp \left\{ -(\mathbf{h}_m - \mathbf{h}_{m,\text{prior}})^H \Sigma_{\mathbf{h}_{m,\text{prior}}}^{-1} (\mathbf{h}_m - \mathbf{h}_{m,\text{prior}}) \right\}$$

where, once more, the receiver requires estimates of the prior parameters of the channel for each transmitter. The outgoing message from variable node  $\mathbf{h}_m$  is obtained by multiplying both incoming messages, leading to

$$n_{\mathbf{h}_m \rightarrow f_O}(\mathbf{h}_m) \propto m_{f_O \rightarrow h_m}(\mathbf{h}_m) m_{f_{C_m} \rightarrow h_m}(\mathbf{h}_m) \propto \exp \left\{ -(\mathbf{h}_m - \hat{\mathbf{h}}_m)^H \hat{\Sigma}_{\mathbf{h}_m}^{-1} (\mathbf{h}_m - \hat{\mathbf{h}}_m) \right\},$$

which equals, up to a proportionality constant, a Gaussian pdf with covariance matrix

$$\hat{\Sigma}_{\mathbf{h}_m} = \left( \hat{\lambda} \hat{\mathbf{X}}_m^H \hat{\mathbf{X}}_m + \hat{\lambda} \hat{\mathbf{D}}_m + \Sigma_{\mathbf{h}_{m,\text{prior}}}^{-1} \right)^{-1}$$

and mean value

$$\hat{\mathbf{h}}_m = \hat{\Sigma}_{\mathbf{h}_m} \left( \hat{\lambda} \hat{\mathbf{X}}_m^H \left( \mathbf{y} - \sum_{m' \neq m} \hat{\mathbf{X}}_{m'} \hat{\mathbf{h}}_{m'} \right) + \Sigma_{\mathbf{h}_{m,\text{prior}}}^{-1} \mathbf{h}_{m,\text{prior}} \right).$$

It is important to note that every time a new message  $n_{\mathbf{h}_m \rightarrow f_O}$  is computed, the set of messages  $\mathbf{M}_C$  needs to be recomputed again, as all  $m_{f_O \rightarrow h_{m'}}, m' \neq m$  depend on the updated messages  $n_{\mathbf{h}_m \rightarrow f_O}$ .

### C. Modulation and Coding Subgraph

The modulation and coding subgraph describes the factor  $f_M$  in (11). We choose to factorize this factor according to

$$f_M(\mathbf{x}, \mathbf{c}, \mathbf{u}) = \prod_{m=1}^M f_{\mathcal{P}_m}(\mathbf{x}_m^{(p)}) f_{\mathcal{M}_m}(\mathbf{x}_m^{(d)}, c_{m,1}, \dots, c_{m,C_m}) f_{\mathcal{C}_m}(c_{m,1}, \dots, c_{m,C_m}, u_{m,1}, \dots, u_{m,U_m}) \prod_{i=1}^{U_m} f_{u_{m,i}}(u_{m,i})$$

where  $f_{\mathcal{P}_m}(\mathbf{x}_m^{(p)}) \triangleq p(\mathbf{x}_m^{(p)})$  denotes the prior pdf of the pilot symbols transmitted from the  $m$ th transmitter,  $f_{\mathcal{M}_m}(\mathbf{x}_m^{(d)}, c_{m,1}, \dots, c_{m,C_m}) \triangleq p(\mathbf{x}_m^{(d)} | c_{m,1}, \dots, c_{m,C_m})$  denotes the modulation constraints on the data symbols of the  $m$ th transmitter,  $f_{\mathcal{C}_m}(c_{m,1}, \dots, c_{m,C_m}, u_{m,1}, \dots, u_{m,U_m}) \triangleq p(c_{m,1}, \dots, c_{m,C_m} | u_{m,1}, \dots, u_{m,U_m})$  represents the code constraints for the  $m$ th codeword and  $f_{u_{m,i}}(u_{m,i}) \triangleq p(u_{m,i})$  is the prior pdf of the  $i$ th information bit transmitted by the  $m$ th antenna. In addition, the vectors  $\mathbf{x}_m^{(p)}$  and  $\mathbf{x}_m^{(d)}$  contain, respectively, the modulated pilot and data symbols transmitted from the  $m$ th antenna. Finally,  $C_m$  and  $U_m$  denote the number of coded and information bits respectively transmitted in a codeword from the  $m$ th antenna. Using this factorization of  $f_M$ , we define the sets  $\mathcal{A}_M$  and  $\mathcal{I}_M$  as

$$\begin{aligned} \mathcal{A}_M &= \{f_{\mathcal{P}_m} | m = 1, \dots, M\} \cup \{f_{\mathcal{M}_m} | m = 1, \dots, M\} \cup \{f_{\mathcal{C}_m} | m = 1, \dots, M\} \\ &\quad \cup \{f_{u_{m,i}} | m = 1, \dots, M, i = 1 \dots U_m\} \\ \mathcal{I}_M &= \{\mathbf{x}_m^{(p)} | m = 1 \dots, M\} \cup \{\mathbf{x}_m^{(d)} | m = 1 \dots, M\} \cup \{c_{m,i} | m = 1, \dots, M, i = 1 \dots C_m\} \\ &\quad \cup \{u_{m,i} | m = 1, \dots, M, i = 1 \dots U_m\}. \end{aligned}$$

The factor graph with the modulation and coding constraints is shown in Fig. 6. As it can be observed, the modulated symbols have been separated into different variable nodes according to the transmit antenna index  $m$  from which they are sent. The symbols corresponding to each transmit antenna port have been further subdivided into two different variable nodes  $\mathbf{x}_m^{(p)}$  and  $\mathbf{x}_m^{(d)}$ , the first containing the pilot symbols and the second containing the modulated data symbols. The modulated data symbols  $\mathbf{x}_m^{(d)}$  are connected to the encoded bits  $c_{m,1}, \dots, c_{m,C_m}$  via the modulation factor node  $f_{\mathcal{M}_m}$ , which describes the mapping of bits onto a complex constellation. The coded bits are, in turn, related to the information bits  $u_{m,1}, \dots, u_{m,U_m}$  through the specific channel code and interleaving scheme utilized, which is represented in a simplified manner by the factor  $f_{\mathcal{C}_m}$  in Fig. 6. Finally, every information bit  $u_{m,i}$  has an associated prior probability represented

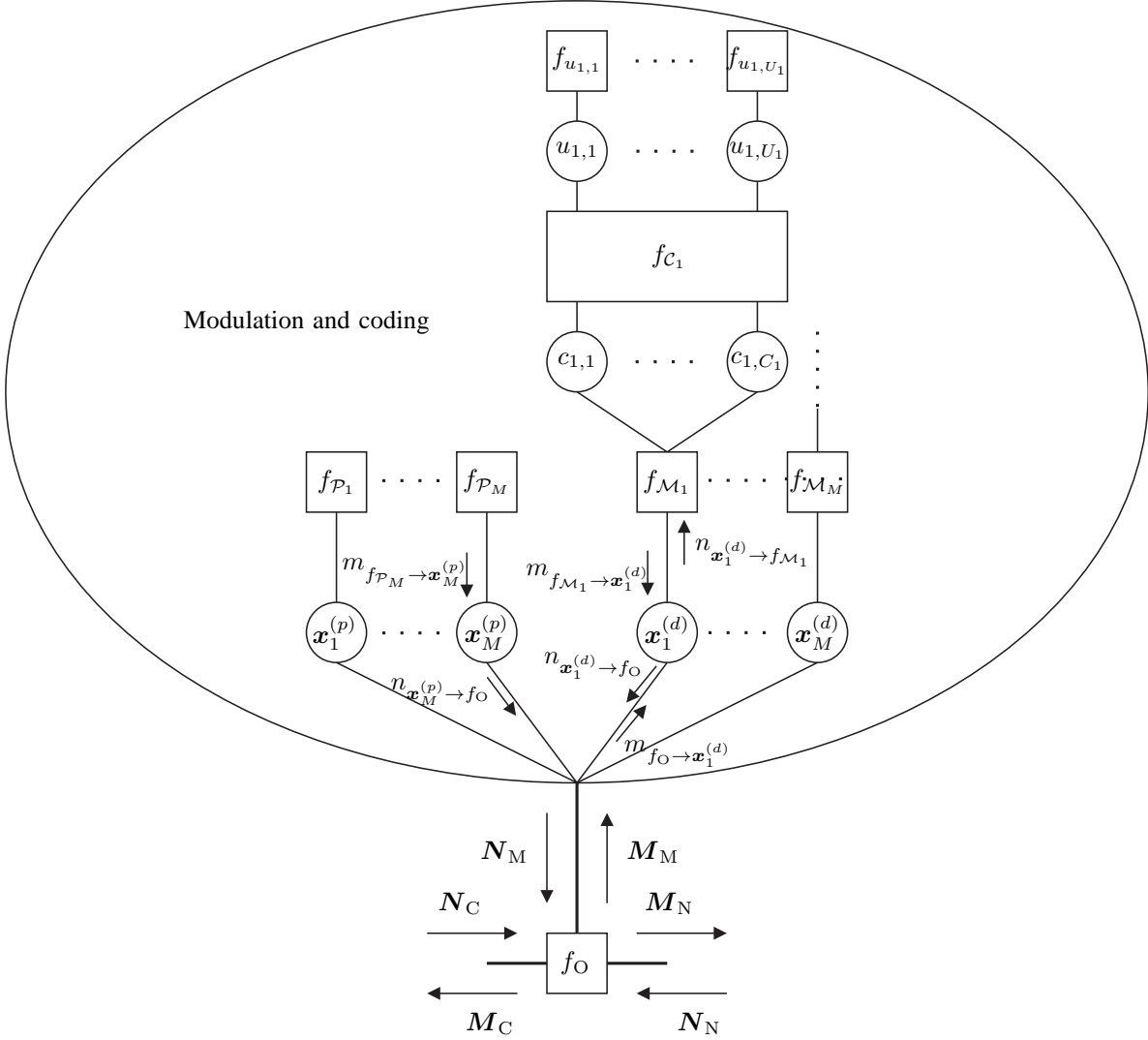


Fig. 6. Subgraph corresponding to the modulation and coding constraints.

by the factor node  $f_{u_{m,i}}$ . For the vast majority of applications, however, the values of the bits will be assumed to be equiprobable. With the proposed structure, the set of incoming messages is defined as  $\mathbf{M}_M = \{m_{f_O \rightarrow \mathbf{x}_m^{(p)}} | m = 1, \dots, M\} \cup \{m_{f_O \rightarrow \mathbf{x}_m^{(d)}} | m = 1, \dots, M\}$ , while the set of outgoing messages becomes  $\mathbf{N}_M = \{n_{\mathbf{x}_m^{(p)} \rightarrow f_O} | m = 1, \dots, M\} \cup \{n_{\mathbf{x}_m^{(d)} \rightarrow f_O} | m = 1, \dots, M\}$ .

In order to ease the derivation of the messages for this subgraph, we can re-write  $f_O(\mathbf{y}, \mathbf{x}, \mathbf{h}, \lambda)$  as

$$f_O(\mathbf{y}, \mathbf{x}, \mathbf{h}, \lambda) \propto \lambda^{KNL} \exp \left\{ -\lambda \left\| \mathbf{y}^{(d)} - \sum_{m=1}^M \mathbf{H}_m^{(d)} \mathbf{x}_m^{(d)} \right\|^2 - \lambda \left\| \mathbf{y}^{(p)} - \sum_{m=1}^M \mathbf{H}_m^{(p)} \mathbf{x}_m^{(p)} \right\|^2 \right\}$$

where the contribution of pilot and data symbols has been split into two separate terms. We start by computing the message that factor node  $f_O$  sends to  $\mathbf{x}_m^{(d)}$ :

$$\begin{aligned} m_{f_O \rightarrow \mathbf{x}_m^{(d)}}(\mathbf{x}_m^{(d)}) &= \exp \left\{ \langle \log f_O(\mathbf{y}, \mathbf{x}, \mathbf{h}, \lambda) \rangle_{N_N N_C N_M^{(m)}} \right\} \\ &\propto \exp \left\{ -\hat{\lambda} \left( \left\| \mathbf{y}^{(d)} - \sum_{m' \neq m} \hat{\mathbf{H}}_{m'}^{(d)} \hat{\mathbf{x}}_{m'}^{(d)} - \hat{\mathbf{H}}_m^{(d)} \mathbf{x}_m^{(d)} \right\|^2 + (\mathbf{x}_m^{(d)})^H \hat{\mathbf{C}}_m^{(d)} \mathbf{x}_m^{(d)} \right. \right. \\ &\quad \left. \left. + \sum_{m' \neq m} \left( (\mathbf{x}_m^{(d)})^H \hat{\mathbf{C}}_{mm'}^{(d)} \hat{\mathbf{x}}_{m'}^{(d)} + (\hat{\mathbf{x}}_{m'}^{(d)})^H (\hat{\mathbf{C}}_{mm'}^{(d)})^H \mathbf{x}_m^{(d)} \right) \right) \right\}. \end{aligned} \quad (14)$$

In the above expression, and similarly to previous definitions,  $\hat{\mathbf{x}}_{m'}^{(d)} = \langle \mathbf{x}_{m'}^{(d)} \rangle_{N_M}$ ,  $\hat{\mathbf{H}}_{m'}^{(d)} = \langle \mathbf{H}_{m'}^{(d)} \rangle_{N_C}$ ,  $\hat{\mathbf{C}}_m^{(d)} = \langle (\mathbf{H}_m^{(d)})^H \mathbf{H}_m^{(d)} \rangle_{N_C} - (\hat{\mathbf{H}}_m^{(d)})^H \hat{\mathbf{H}}_m^{(d)}$  and  $\hat{\mathbf{C}}_{mm'}^{(d)} = \langle (\mathbf{H}_m^{(d)})^H \mathbf{H}_{m'}^{(d)} \rangle_{N_C} - (\hat{\mathbf{H}}_m^{(d)})^H \hat{\mathbf{H}}_{m'}^{(d)}$ . Additionally,  $\mathbf{N}_M^{(m)} = \{n_{\mathbf{x}_i^{(p)} \rightarrow f_O} | i = 1, \dots, M\} \cup \{n_{\mathbf{x}_i^{(d)} \rightarrow f_O} | i = 1, \dots, M, i \neq m\}$  denotes the set of all outgoing detection messages except  $n_{\mathbf{x}_m^{(d)} \rightarrow f_O}$ . The message in (14) is proportional to a Gaussian pdf with covariance matrix

$$\hat{\Sigma}_{\mathbf{x}_m^{(d)}, \text{VMP}} = \hat{\lambda}^{-1} \left( (\hat{\mathbf{H}}_m^{(d)})^H \hat{\mathbf{H}}_m^{(d)} + \hat{\mathbf{C}}_m^{(d)} \right)^{-1}$$

and mean

$$\hat{\mathbf{x}}_{m, \text{VMP}}^{(d)} = \hat{\lambda} \hat{\Sigma}_{\mathbf{x}_m^{(d)}, \text{VMP}} \left( (\hat{\mathbf{H}}_m^{(d)})^H \left( \mathbf{y}^{(d)} - \sum_{m' \neq m} \hat{\mathbf{H}}_{m'}^{(d)} \hat{\mathbf{x}}_{m'}^{(d)} \right) - \sum_{m' \neq m} \hat{\mathbf{C}}_{mm'}^{(d)} \hat{\mathbf{x}}_{m'}^{(d)} \right).$$

The outgoing message  $n_{\mathbf{x}_m^{(d)} \rightarrow f_O}(\mathbf{x}_m^{(d)})$  is obtained by multiplying the messages  $m_{f_O \rightarrow \mathbf{x}_m^{(d)}}(\mathbf{x}_m^{(d)})$  and  $m_{f_{\mathcal{M}_m} \rightarrow \mathbf{x}_m^{(d)}}$ . In this case,  $m_{f_{\mathcal{M}_m} \rightarrow \mathbf{x}_m^{(d)}}$  is a SP message reading

$$m_{f_{\mathcal{M}_m} \rightarrow \mathbf{x}_m^{(d)}} \propto \prod_{i=1}^{N_d} \left( \sum_{s \in \mathcal{S}_m} \beta_{x_m^{(d)}(i)}(s) \delta(x_m^{(d)}(i) - s) \right) \quad (15)$$

where  $\mathcal{S}_m$  is the modulation set for user  $m$  and  $\beta_{x_m^{(d)}(i)}(s)$  represents the extrinsic values of  $x_m^{(d)}(i)$  for each constellation point  $s \in \mathcal{S}_m$ , obtained from the SP demodulator and decoder. The combined message fed back to the observation factor node reads

$$\begin{aligned} n_{\mathbf{x}_m^{(d)} \rightarrow f_O}(\mathbf{x}_m^{(d)}) &\propto m_{f_O \rightarrow \mathbf{x}_m^{(d)}}(\mathbf{x}_m^{(d)}) m_{f_{\mathcal{M}_m} \rightarrow \mathbf{x}_m^{(d)}}(\mathbf{x}_m^{(d)}) \\ &\propto \prod_{i=1}^{N_d} \left( \sum_{s \in \mathcal{S}_m} \beta_{x_m^{(d)}(i)}(s) \exp \left\{ \frac{-|s - \hat{x}_{m, \text{VMP}}^{(d)}(i)|^2}{\sigma_{x_m^{(d)}(i)}^2} \right\} \delta(x_m^{(d)}(i) - s) \right), \end{aligned} \quad (16)$$

where  $\sigma_{x_m^{(d)}(i)}^2$  is the  $i$ th entry in the main diagonal of  $\hat{\Sigma}_{\mathbf{x}_m^{(d)}, \text{VMP}}$ . It can be observed that the message factorizes with respect to the individual modulated symbols  $x_m^{(d)}(i)$ , so the mean and variance

of each data symbol can be computed independently and used to build the mean vector  $\hat{\mathbf{x}}$  and the covariance matrix  $\hat{\Sigma}_{\mathbf{x}}$  by inserting the updated mean and variances in their corresponding positions.

It is important to note that, because the factor node  $f_{\mathcal{M}_m}$  is a SP factor node, the message  $n_{\mathbf{x}_m^{(d)} \rightarrow f_{\mathcal{M}_m}}$  is obtained by multiplying all messages received at variable node  $\mathbf{x}_m^{(d)}$  except the message coming from  $f_{\mathcal{M}_m}$ , which in this particular setup reduces to

$$n_{\mathbf{x}_m^{(d)} \rightarrow f_{\mathcal{M}_m}}(\mathbf{x}_m^{(d)}) = m_{f_{\mathcal{O}} \rightarrow \mathbf{x}_m^{(d)}}(\mathbf{x}_m^{(d)}).$$

All message-passing among the modulation factor nodes, coded bits and information bits is completed by using the standard SP algorithm, and will therefore not be described here.

It remains to describe the income and outcome messages involving pilot symbols. As pilot symbols are known by the receiver, their prior distribution is  $p(x_m^{(p)}(i)) = \delta(x_m^{(p)}(i) - p_m(i))$  with  $p_m(i)$  denoting the  $i$ th pilot symbol sent from transmit antenna  $m$ . This imposes that the outgoing message  $n_{\mathbf{x}_m^{(p)} \rightarrow f_{\mathcal{O}}}$  is also a Dirac delta, which can also be described as a degenerate Gaussian message with mean  $\hat{\mathbf{x}}_m^{(p)} = \mathbf{p}_m$  and covariance  $\hat{\Sigma}_{\mathbf{x}_m^{(p)}} = \mathbf{0}$ .

## V. SIMULATION RESULTS

In this section, we propose a number of receiver structures based on the derivations made in Section IV and evaluate their performance by means of Monte-Carlo simulations. First, we present the parameters of the MIMO-OFDM system considered, followed by a description of the specific receiver structures that will be evaluated. Finally, the BER performance results obtained are presented and discussed.

### A. Description of the MIMO-OFDM System

We begin by describing the MIMO-OFDM system used for obtaining the numerical results. Its main parameters are summarized in Table I. We consider an OFDM system with  $M = N = 2$  antennas at both transmitter and receiver ends. Two streams of random bits are independently encoded using a convolutional code with rate 1/3 and generating polynomials 133, 171 and 165 (octal). After channel interleaving, the coded bits are mapped onto symbols of a QPSK or 16QAM constellation (with Gray mapping) which are then inserted into an OFDM frame consisting of  $L = 7$  OFDM symbols with  $K = 75$  subcarriers and with a subcarrier spacing of

TABLE I  
PARAMETERS OF THE SIMULATED OFDM SYSTEM

Parameter	Value
Tx antennas ( $M$ )	2
Rx antennas ( $N$ )	2
Subcarriers ( $K$ )	75
OFDM symbols ( $L$ )	7
Subcarrier spacing ( $\Delta f$ )	15 kHz
Channel coding	1/3 Convolutional
Symbol mapping	16QAM
Pilot symbols	13
Channel model	3GPP ETU

15kHz. Part of the time-frequency elements are reserved for the transmission of pilot symbols. We specify the following pilot patterns: pilot symbols are transmitted in the first and fifth OFDM symbol of the frame, with a frequency spacing of 12 subcarriers, resulting in a total of 13 pilot symbols per frame. Note that both transmit antennas share the same time-frequency elements for the simultaneous transmission of pilot symbols. Pilot symbols are randomly chosen from a QPSK constellation.

Realizations of the channel time-frequency response are randomly generated using the extended typical urban (ETU) model from the 3GPP LTE standard [44] with 9 Rayleigh-fading taps. The channel responses corresponding to two different transmitters are uncorrelated and remain static over the duration of an OFDM frame. A new channel response is generated for each OFDM frame, with the responses of two different frames being also uncorrelated.

### B. Receiver Structures

We introduce now the specific receiver architectures that will be evaluated in this section. All receivers are based on the generic message-passing receiver presented in Section IV. The messages exchanged can be obtained by particularizing the generic messages according to the specific receiver configuration, as it will be detailed in the following. We evaluate three main types of VMP-SP receiver, which are described next.

1) *I-DJC-DD and I-DSC-DD Receivers*: First, we introduce a full iterative receiver using exactly the messages derived in Section IV. The receiver operates by iteratively updating the

beliefs of the channel weight vector, the data symbols and information bits and, finally, the noise precision parameter.

Initialization of the beliefs of the channel weights and the transmitted symbols is required. The initialization of the channel weights is obtained from a pilot-based joint linear minimum mean-squared-error (LMMSE) channel estimator. For the initialization of the transmitted symbols, maximum-likelihood detection (MLD) is used, followed by soft-in soft-out (SISO) BCJR decoding. The belief of the transmitted data symbols is set to a Gaussian pdf with mean and covariance values obtained from soft modulation of the a-posteriori probabilities (APP) of the coded bits obtained from the SISO BCJR decoder. An initial estimate of the noise precision is obtained as in Section IV-A. After the initialization, a full iteration of the receiver consists of updating the beliefs of the channel weight vectors (using either the joint channel weight model in Fig. 4 or the disjoint channel weight model in Fig. 5), a message-passing run on the modulation and coding subgraph (updating the beliefs of transmitted symbols, coded bits and information bits) and, finally, an update of the noise precision parameter. Note that the message-passing operations done through the channel code factor node can be replaced by SISO BCJR decoding. In this case, the SP messages  $n_{c_m,k \rightarrow f_{\mathcal{M}_m}}$  can be identified to be the extrinsic values of the coded bits output by the BCJR decoder.

We refer to the described architectures as Iterative - Data-aided Joint Channel estimation - Data Decoding (I-DJC-DD) for the receiver using the joint channel weights model and Iterative - Data-aided Sequential Channel estimation - Data Decoding (I-DSC-DD) for the receiver obtained using the disjoint channel weights model.

2) *DJC-DD and DSC-DD Receivers*: We introduce now a class of receivers which perform iterative data-aided channel weights and noise precision estimation together with equalization and demodulation of the transmitted symbols. Compared to the receivers presented before, channel decoding is left outside of the iterative process, and is performed only once at the end after convergence of the algorithm. The receiver capitalizes on just the knowledge of the complex modulation structure of the transmitted signal to refine its channel estimates, and not on the code structure. This receiver architecture is obtained by applying a special scheduling to the message computation and exchange between the subgraphs. Specifically, no messages are passed from variable nodes  $\mathbf{x}_m^{(d)}$  to factor nodes  $f_{\mathcal{M}_m}$  until the last iteration of the algorithm. Instead, after

the messages  $m_{f_O \rightarrow x_m^{(d)}}$  are computed, the updated message  $n_{x_m^{(d)} \rightarrow f_O}$  is directly computed using (16). To this end, an initial value of the messages  $m_{f_{\mathcal{M}_m} \rightarrow x_m^{(d)}}$  is needed. This can be obtained by setting

$$\beta_{x_m^{(d)}(i)}(s) = \frac{1}{|\mathcal{S}_m|} \quad \forall m = 1, \dots, M, i = 1, \dots, N_d, s \in \mathcal{S}_m$$

in (15). In the expression above,  $|\mathcal{S}_m|$  denotes the cardinality of the set  $\mathcal{S}_m$ . Note that this initialization corresponds to assuming that all modulated symbols in the constellation are equally likely, which is a valid assumption when the information bits are equiprobable and the channel code is regular.

As for the previous receivers, an initialization of the beliefs of the channel weight vector, noise precision and transmitted symbols is required. The channel weight vectors are initialized as a Gaussian pdf, with mean obtained from a pilot-based LMSSE channel estimator and null covariance. Similarly, the beliefs of the transmitted symbols are also set to a Gaussian pdf with mean and covariance values obtained from a MIMO MLD (no BCJR decoding is done, as opposed to the I-DJC-DD and I-DSC-DD receivers). An initial estimate of the noise precision is then obtained following the procedure in Section IV-A. After the initialization, the receiver operates by iteratively updating the beliefs of the channel weights (either jointly as in Fig. 4, or sequentially as in Fig. 5), the transmitted symbols and noise precision parameter. After convergence of the algorithm (or maximum number of iterations attained), the messages  $n_{x_m^{(d)} \rightarrow f_{\mathcal{M}_m}}$  are computed, and a round of decoding based on the SP algorithm is performed, yielding the beliefs of the information bits.

We refer to these receivers as Data-aided Joint Channel estimation - Data Decoding (DJC-DD) for the receiver using the joint channel weight prior model (Section IV-B1) and Data-aided Sequential Channel estimation - Data Decoding (DSC-DD) for the receiver using the disjoint channel weight prior model (Section IV-B2).

3) *PSC-DD Receiver*: Finally we present a simple receiver consisting of a pilot-aided channel estimator, a MIMO maximum likelihood detector (MLD) and data decoding. The channel estimation module is based on the VMP-SP generic receiver described in Section IV. It updates iteratively the beliefs of the channel weight vectors corresponding to each transmit antenna and the noise precision. To this end, the channel estimator only exploits the pilot signals transmitted from each transmit antenna and does not capitalize on data symbols to refine its estimates.

In order to obtain this pilot-aided channel estimator from the generic receiver architecture in Section IV, the messages  $n_{\mathbf{x}_m^{(d)} \rightarrow f_{\text{O}}}$  must be set to

$$n_{\mathbf{x}_m^{(d)} \rightarrow f_{\text{O}}}(\mathbf{x}_m^{(d)}) = \prod_i \delta(x_m^{(d)}(i)).$$

This enforces that data symbols are not employed for channel weight estimation. In addition, the disjoint channel weights setup (see Fig. 5) is selected. With this configuration, the output messages  $N_{\text{M}}$  are constant, reflecting the receiver's knowledge on the value of the pilot symbols. Hence, expectations taken over  $N_{\text{M}}$  in the channel weights and noise precision subgraphs reduce to the value of the pilot symbols (or zero for data symbols), with all second-order terms vanishing. Note that, for this channel estimator, no update of the beliefs of the data symbols is performed. Equalization and decoding are done outside the VMP-SP framework.

Additionally, a small modification in the processing corresponding to the noise precision subgraph is required. Note that, for the computation of the message  $m_{f_{\text{O}} \rightarrow \lambda}$ , the signal received at all –pilot and data– subcarriers is used, while only the signals received at pilot positions are utilized for channel weight estimation. This can be avoided by restricting this message to include only the observation at pilot positions, i.e. calculating  $m_{f_{\text{O}^{(p)}} \rightarrow \lambda}$  instead, where

$$f_{\text{O}^{(p)}}(\mathbf{y}^{(p)}, \mathbf{x}^{(p)}, \mathbf{h}^{(p)}, \lambda) \triangleq p(\mathbf{y}^{(p)} | \mathbf{x}^{(p)}, \mathbf{h}^{(p)}, \lambda) \propto \lambda^{N^{(p)}} \exp \left\{ -\lambda \left\| \mathbf{y}^{(p)} - \mathbf{X}^{(p)} \mathbf{h}^{(p)} \right\|^2 \right\},$$

with  $N^{(p)}$  denoting the total number of pilots in a frame.

The initialization for this estimator is simpler compared to that of the other receivers. It consists of setting the beliefs of the channel weight vector corresponding to each transmit antenna to a Gaussian prior with zero mean and zero covariance, while an initial value for the noise precision can be obtained from the signal received at pilot subcarriers. The receiver operates by sequentially updating the channel weight vectors corresponding to each transmitter  $\mathbf{h}_1, \dots, \mathbf{h}_M$  following the procedure described in Section IV-B2. This is followed by an update of the noise precision parameter. The channel responses belonging to each transmit antenna obtained after convergence of the iterative estimator are fed to a MIMO maximum likelihood detector (MLD), followed by BCJR decoding. Thus, we can obtain BER performance results and benchmark them with analogous receiver structures using a different channel estimator.

As we will see in the performance evaluation, this iterative estimator approximates the performance of a pilot-based joint LMMSE channel estimator with perfect knowledge of the noise

TABLE II  
SUMMARY OF RECEIVER STRUCTURES

Receiver	Initialization		Operation	
	Channel Weights	Transmitted Symbols	Channel Weight Model	Demodulation & Decoding
PSC-DD	Null mean and covariance	–	Disjoint	–
DJC-DD	LMMSE estimator	ML detector	Joint	Demodulation only
DSC-DD	LMMSE estimator	ML detector	Disjoint	Demodulation only
I-DJC-DD	LMMSE estimator	MLD + BCJR	Joint	Demodulation and decoding
I-DSC-DD	LMMSE estimator	MLD + BCJR	Disjoint	Demodulation and decoding

variance. The iterative estimator, however, presents the advantage of avoiding cumbersome matrix inversions depending on the specific values of the pilot-symbols. This estimator was presented (outside the context of message-passing techniques) in [34]. A more detailed discussion of the computational advantages of this estimator over the LMMSE estimator is provided in this contribution.

In the following, we refer to this receiver as Pilot-aided Sequential Channel estimation - Data Decoding (PSC-DD) receiver.

The main characteristics of all the receivers presented above are summarized in Table II.

### C. Numerical Results

We evaluate separately the performance of the three architectures described in Section V-B, beginning with the simplest scheme, the PSC-DD receiver; we follow with the DJC-DD and DSC-DD receivers and conclude with the most advanced structures: the I-DJC-DD and I-DSC-DD receivers.

In Fig. 7, the mean squared error (MSE) of the estimates of the channel weights obtained with the PSC-DD receiver is depicted. The MSE is plotted for three different  $E_b/N_0$  values as a function of the number of iterations performed. It is observed that the performance of the sequential pilot-based estimator approaches the performance of a joint LMMSE estimator with sufficient number of iterations. It is especially interesting to note the dependency of the number of iterations required for convergence on the  $E_b/N_0$  value. For  $E_b/N_0 = -2\text{dB}$  and  $E_b/N_0 = 2\text{dB}$ , between 2 and 3 iterations are sufficient to achieve an MSE virtually equal to the LMMSE bound. When increasing  $E_b/N_0$  to 6dB, however, a minimum number of 5 iterations

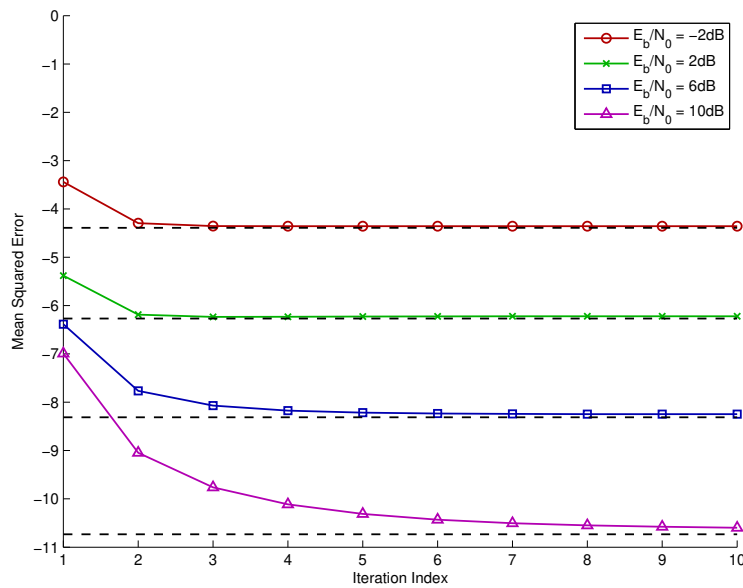


Fig. 7. MSE of the estimates of the channel weights for the PSC-DD receiver versus the iteration index. 13 pilot symbols are inserted per OFDM frame. The dashed black lines represent the MSE obtained with pilot-based LMMSE joint channel estimation.

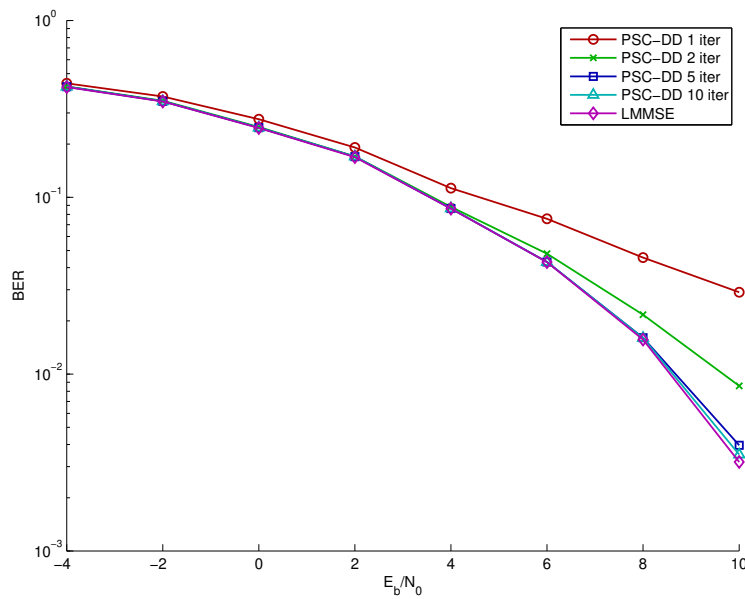


Fig. 8. BER as a function of  $E_b/N_0$  for the PSC-DD receiver with QPSK modulation. 13 pilot symbols are inserted per OFDM frame. The BER performance of a similar receiver using LMMSE channel estimation with knowledge of the noise variance is included as a reference.

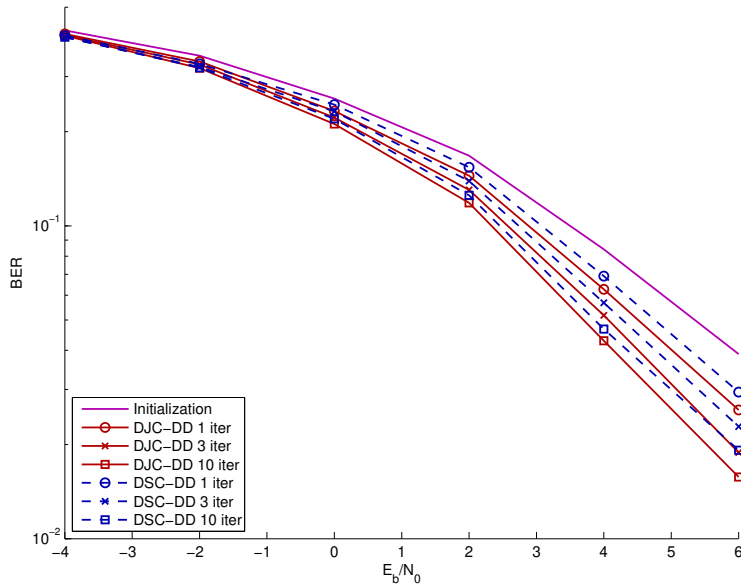


Fig. 9. BER as a function of  $E_b/N_0$  for the DJC-DD and DSC-DD receivers with QPSK modulation. 13 pilot symbols are inserted per OFDM frame.

is needed, and about 10 iterations are required for  $E_b/N_0 = 10$ dB. Similar observations can be made when evaluating the BER of the receiver with QPSK modulation, as shown in Fig. 8. Again, the performance of the PSC-DD receiver equals that of the receiver with the LMMSE estimator when enough iterations for the receiver to converge have been run, and fewer iterations are needed the smaller  $E_b/N_0$  is. These results suggest that the iterative channel estimator in the PSC-DD receiver would be a good choice to obtain an initial channel estimate for the more complex iterative structures that we will discuss next. Furthermore, this channel estimator has the additional benefit of outputting soft estimates (the beliefs) of both the channel weights and the noise precision. Classical channel estimators, on the other hand, typically require separate noise estimation prior to the estimation of the channel weights, and only provide hard (point) estimates.

BER results for the DJC-DD and DSC-DD receivers are portrayed in Fig. 9. The results have been obtained using a QPSK constellation for the modulation of data symbols. They indicate that a significant performance gain can be obtained by iteratively updating the channel weights, transmitted data symbols and noise precision parameter after the initialization, even though the receiver does not capitalize on the code structure within the iterative process. For both

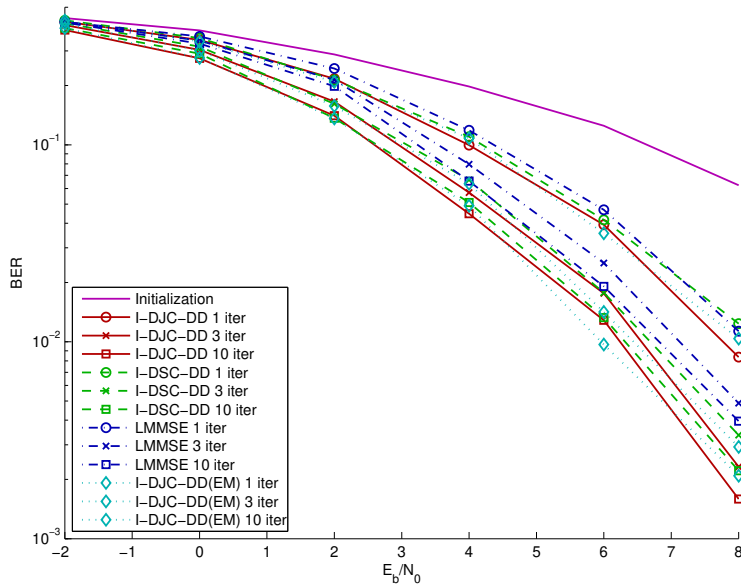


Fig. 10. BER as a function of  $E_b/N_0$  for the I-DJC-DD and I-DSC-DD receivers with 16-QAM modulation. 13 pilot symbols are inserted per OFDM frame.

receivers (with joint and sequential channel estimation), most of the improvement with respect to the initialization is obtained in the first three iterations, with only marginal gains obtained after further processing. Regarding the channel estimation approach, DJC-DD leads to a slightly better performance than DSC-DD in the whole simulated  $E_b/N_0$  range; the improved accuracy of the joint estimation approach comes at the expense of a larger computational complexity, as it operates with vectors and matrices of dimensions  $M$  times as large as in the sequential estimation approach, which can be a problem when calculating the necessary matrix inversions.

Note that the receivers evaluated in Fig. 9 operate by capitalizing on the structure of the constellation used for the modulation of data symbols. Hence, their performance strongly depends on the type of modulation used. Low-order modulations, such as BPSK or QPSK, favor this receiver, as there is a relatively large distance between the points in the constellation, allowing better refining (through SP message-passing) of the VMP estimates of the transmitted symbols. When using higher order modulations, however, the receiver's performance suffers from the relatively small distance between adjacent constellation points. Specifically for the system investigated in this work, we found that the DJC-DD and DSC-DD receivers for 16-QAM or higher order modulations do not improve the performance with respect to the initialization.

The aforementioned problem with high-order modulations can be circumvented with the inclusion of the channel code structure in the iterative processing, as done in the I-DJC-DD and I-DSC-DD receivers. The BER performance of both receivers with 16-QAM modulated data symbols is depicted in Fig. 10. For benchmarking purposes, the BER performance of a heuristically designed iterative receiver with analogous features to the I-DJC-DD receiver is also plotted. We refer to this receiver as LMMSE receiver, as the channel estimation and MIMO detection modules are separately designed after the LMMSE principle. The LMMSE receiver is based on the design proposed in [9] for a multiuser CDMA receiver, and was adapted to MIMO-OFDM in [40], where a detailed description of its operational principles can be found. In addition, the BER performance of a modified version of the I-DJC-DD receiver has also been included. This receiver, which we denote as I-DJC-DD(EM) receiver, results from applying the EM restriction to the beliefs of the channel weights  $\mathbf{h}$  and the noise precision parameter  $\lambda$ . Thus, this receiver is identical to the I-DJC-DD receiver except that the messages  $n_{\mathbf{h} \rightarrow f_O}$  and  $n_{\lambda \rightarrow f_O}$  are computed according to (7). This modified messages imply that all terms depending on the second order moments of  $b_{\mathbf{h}} = n_{\mathbf{h} \rightarrow f_O}$  vanish.

The results show that vast improvements in BER of the I-DJC-DD and I-DSC-DD receivers with respect to the initialization are obtained, even for very low  $E_b/N_0$  values. As in the case of the DJC-DD and DSC-DD receivers, joint estimation of the channel weights performs marginally better than sequential estimation. Both message-passing receivers clearly outperform the heuristic LMMSE receiver, with  $E_b/N_0$  gains close to 1dB at a BER of 1%. We explain these gains by the fact that, contrary to the separate design of the different modules in the LMMSE receiver, our VMP-SP receivers are analytically derived based on a global objective function, namely the region-based free energy. This global design ensures that the information shared by the different receiver components is treated correctly, and resolves the choice of the appropriate type of information to be passed from the channel decoder to the other component parts of the receiver. It is also remarkable that the EM-constrained version of the I-DJC-DD receiver achieves roughly the same performance as the non-constrained version. This result seems to indicate that there is no significant gain to be achieved by computing soft channel estimates as compared to just point estimates, at least for the system considered.

Another key feature of the I-DJC-DD and I-DSC-DD receivers is the estimation of the noise precision. This functionality does not only account for the AWGN, but also includes inaccuracies

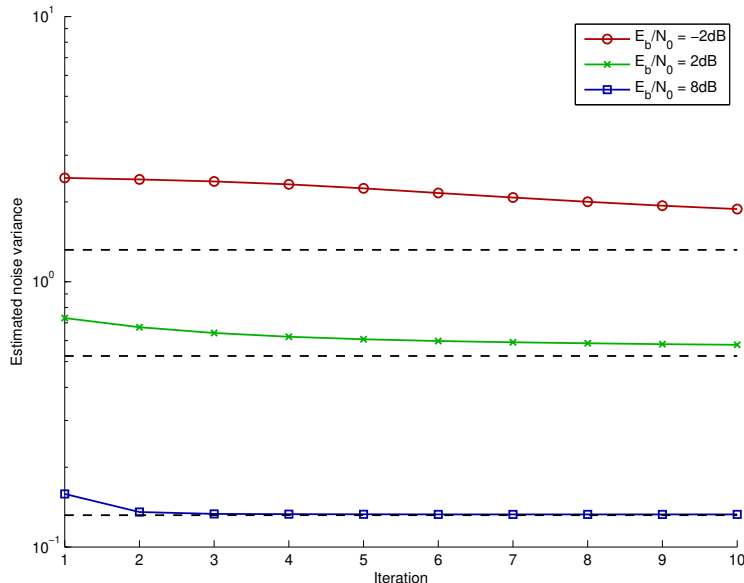


Fig. 11. Average noise variance estimated by the I-DJC-DD receiver as a function of the iteration index. 13 pilot symbols are inserted per OFDM frame. The dashed black lines represent the true noise variance for each  $E_b/N_0$  value.

in the estimates of the channel weights and data symbols. Fig. 11 depicts the averaged noise variance estimate (inverse of the noise precision estimate  $\lambda$ ) provided by the I-DJC-DD receiver as a function of the iteration index for three different  $E_b/N_0$  levels. The true AWGN variances are also depicted as dashed black lines. It is apparent from the results that the behavior of the noise variance estimates (with respect to the true value) depends heavily on the regime in which the receiver is operating. For the very low  $E_b/N_0$  regime, the receiver significantly overestimates the noise variance; this is due to the low accuracy of the channel weights estimates and the large amount of errors in the estimates of the data symbols obtained. At the other extreme, for high  $E_b/N_0$  values, the estimates of the channel weights and data symbols become so accurate (as it can be observed from the low BER values) that the noise variance estimate rapidly converges to the true AWGN variance, as the contribution of the estimates' inaccuracies becomes negligible. In the medium  $E_b/N_0$  range, the noise variance estimate slowly converges to a value larger than the true variance, the difference between both values depending again on the accuracy of the other parameters' estimates.

Conceptually, the estimate of the noise precision represents the amount of 'trust' that the algorithm has on the beliefs of the channel weights and data symbols. With high noise precision

values, the receiver has high confidence on these beliefs, leading to a rapid convergence towards a stable solution. On the contrary, low noise precision values will yield slower changes on the beliefs from one iteration to the next, resulting in a slower convergence rate.

## VI. CONCLUSION

In this article we have used a hybrid VMP-SP message passing framework [41], [42] for the design of iterative receivers for wireless communication. The framework has been applied to the factor graph of a generic MIMO-OFDM system. The messages obtained from the generic derivation have been used to obtain a set of receiver architectures ranging from computationally simple solutions to full-scale iterative architectures performing channel weight estimation, noise precision estimation, MIMO equalization and channel decoding. The performance of the proposed receivers has been assessed and compared to state-of-the-art solutions via Monte Carlo simulations.

A fundamental contribution of this work is the application of a unified framework that jointly optimizes the receiver architecture based on a global cost function, namely the region-based variational free energy. The message-passing scheme used in this work can be obtained from the equations of the stationary points of a particular region-based free energy approximation. The resulting algorithm applies the VMP and SP algorithms to different parts of the graph and unequivocally defines how the messages of the two respective frameworks are to be combined. As a result, the hybrid technique allows for a convenient design of wireless receivers in which the SP algorithm is used for demodulation and channel decoding and the VMP algorithm is applied for channel weight estimation, noise covariance estimation and MIMO equalization. The connection between the specific receiver component parts is defined by the message-computation rules, in contrast to other approaches in which the selection of information to be exchanged among the specific receiver components is done based on numerical results and/or intuitive argumentation.

We illustrate the application of the framework by applying it to the design of receivers in a MIMO-OFDM communications system. From the factor-graph representing the underlying probabilistic model, a set of generic messages exchanged between different parts of the model, represented by sub-graphs, is derived. We choose to split the factor graph in three main subgraphs corresponding to the channel weights prior model, the noise precision model and the modulation and coding constraints. The advantage of this modular approach is that it enables a scalable,

flexible design of the receiver in which the modification of a specific sub-graph does not modify the processing performed in other parts of the graph. Thus, a collection of different receiver architectures can be obtained by applying different initialization and scheduling strategies.

In order to assess the performance of the receivers derived with the proposed framework, we define five specific instances of the generic message-passing receiver. The particular architectures selected span from to full-scale iterative schemes, in which the output of the channel decoder is used to refine the estimates of the channel parameters and the transmitted symbols, to low-complexity solutions, in which only pilot symbols are used for channel weight and noise variance estimation. This particular selection of receiver architectures serves as an illustration of how the tradeoff between computational complexity and receiver performance can be adjusted, with the generic message-passing receiver as a starting point. The numerical results, obtained via Monte Carlo simulations in a realistic MIMO-OFDM setup, confirm the effectiveness of the receivers derived following the hybrid VMP-SP framework. In particular, the convergence behavior of the receivers tested is especially remarkable. All receiver instances yield an improved or equal performance with increasing number of iterations, both in terms of BER and MSE of the channel weight estimates. We explain these favorable convergence properties by the use of the unique, global cost function from which the algorithm is derived. The estimation of the noise precision parameter, accounting for the uncertainty on the estimates of the channel weights and transmitted symbols in addition to the AWGN variance, is another key feature of the proposed architecture.

## REFERENCES

- [1] D. Gesbert, M. Shafi, D.-S. Shiu, P. Smith, and A. Naguib, "From theory to practice: an overview of MIMO space-time coded wireless systems," *IEEE J. Select. Areas Commun.*, vol. 21, no. 3, pp. 281–302, Apr. 2003.
- [2] C. Berrou, A. Glavieux, and P. Thitimajshima, "Near Shannon limit error-correcting coding and decoding: Turbo codes," in *Proc. IEEE International Conference on Communications, (ICC'93)*, May 1993, pp. 1064–1070.
- [3] R. Gallager, "Low-density parity-check codes," *IEEE Trans. Inform. Theory*, vol. 8, no. 1, pp. 21–28, Jan. 1962.
- [4] E. Telatar, "Capacity of multi-antenna Gaussian channels," *European Transactions on Telecommunications*, vol. 10, pp. 585–595, 1999.
- [5] L. Zheng and D. N. C. Tse, "Diversity and multiplexing: a fundamental tradeoff in multiple-antenna channels," *IEEE Trans. Inform. Theory*, vol. 49, pp. 1073–1096, May 2003.
- [6] X. Wang and H. Poor, "Iterative (turbo) soft interference cancellation and decoding for coded CDMA," *IEEE Trans. Commun.*, vol. 47, pp. 1046–1061, Jul. 1999.
- [7] R. Koetter, A. C. Singer, and M. Tücher, "Turbo equalization," *IEEE Signal Processing Mag.*, vol. 21, pp. 67–80, Jan. 2004.

- [8] M. Lončar, R. Müller, J. Wehinger, C. Mecklenbräuker, and T. Abe, “Iterative channel estimation and data detection in frequency-selective fading MIMO channels,” *European Transactions on Telecommunications*, vol. 15, pp. 459–470, Sep. 2004.
- [9] J. Wehinger and C. Mecklenbräuker, “Iterative CDMA multiuser receiver with soft decision-directed channel estimation,” *IEEE Trans. Signal Processing*, vol. 54, pp. 3922–3934, Oct. 2006.
- [10] P. Rossi and R. Müller, “Joint twofold-iterative channel estimation and multiuser detection for MIMO-OFDM systems,” *IEEE Trans. Wireless Commun.*, vol. 7, no. 11, pp. 4719–4729, Nov. 2008.
- [11] M. Wainwright and M. Jordan, “Graphical models, exponential families, and variational inference,” *Foundations and Trends in Machine Learning*, vol. 1, no. 1-2, pp. 1–305, Dec. 2008.
- [12] J. Winn and C. Bishop, “Variational message passing,” *Journal of Machine Learning Research*, vol. 6, pp. 661–694, 2005.
- [13] C. Bishop, *Pattern Recognition and Machine Learning*. Springer, 2006.
- [14] J. Yedidia, W. Freeman, and Y. Weiss, “Constructing free-energy approximations and generalized belief propagation algorithms,” *IEEE Trans. Inform. Theory*, vol. 51, no. 7, pp. 2282–2312, Jul. 2005.
- [15] T. Minka, “Divergence measures and message passing,” *Microsoft Research Cambridge UK Technical Report*, vol. 72, no. TR-2005-173, 2005.
- [16] J. Pearl, *Probabilistic reasoning in intelligent systems: networks of plausible inference*. Morgan Kaufmann, 1988.
- [17] F. Kschischang, B. Frey, and H.-A. Loeliger, “Factor graphs and the sum-product algorithm,” *IEEE Trans. Inform. Theory*, vol. 47, no. 2, pp. 498–519, Feb. 2001.
- [18] K. P. Murphy, Y. Weiss, and M. I. Jordan, “Loopy belief propagation for approximate inference: an empirical study,” in *Proceedings of uncertainty in artificial intelligence*, 1999, pp. 467–475.
- [19] R. McEliece, D. MacKay, and J. Cheng, “Turbo decoding as an instance of Pearl’s belief “propagation” algorithms,” *IEEE J. Select. Areas Commun.*, vol. 16, no. 2, pp. 140–152, Feb. 1998.
- [20] J. Boutros and G. Caire, “Iterative multiuser joint decoding: unified framework and asymptotic analysis,” *IEEE Trans. Inform. Theory*, vol. 48, no. 7, pp. 1772–1793, Jul 2002.
- [21] H.-A. Loeliger, J. Dauwels, J. Hu, S. Korl, L. Ping, and F. Kschischang, “The factor graph approach to model-based signal processing,” *Proc. IEEE*, vol. 95, no. 6, pp. 1295–1322, Jun. 2007.
- [22] G. Colavolpe and G. Germi, “On the application of factor graphs and the sum-product algorithm to ISI channels,” *IEEE Trans. Commun.*, vol. 53, no. 5, pp. 818–825, 2005.
- [23] C. Novak, G. Matz, and F. Hlawatsch, “A factor graph approach to joint iterative data detection and channel estimation in pilot-assisted IDMA transmissions,” in *Proc. IEEE International Conference on Acoustics, Speech and Signal Processing (ICASSP 2008)*, Apr. 2008, pp. 2697–2700.
- [24] A. P. Worthen and W. E. Stark, “Unified design of iterative receivers using factor graphs,” *IEEE Trans. Inform. Theory*, vol. 47, no. 2, pp. 843–849, Feb. 2001.
- [25] T. Moon, “The expectation maximization algorithm,” *IEEE Signal Processing Mag.*, vol. 13, pp. 47–60, Nov. 1996.
- [26] C. Novak, F. Hlawatsch, and G. Matz, “Low-complexity factor graph receivers for spectrally efficient MIMO-IDMA,” in *Proc. IEEE International Conference on Communications (ICC’08)*, may 2008, pp. 770 –774.
- [27] C. Novak, G. Matz, and F. Hlawatsch, “Factor graph based design of an OFDM-IDMA receiver performing joint data detection, channel estimation, and channel length selection,” in *Proc. IEEE International Conference on Acoustics, Speech and Signal Processing (ICASSP 2009)*, Apr. 2009, pp. 2561–2564.

- [28] H. Attias, “Inferring parameters and structure of latent variable models by variational Bayes,” in *Proceedings of the Fifteenth Conf. on Uncertainty in Artificial Intelligence*, 1999, pp. 21–30.
- [29] M. Beal, “Variational algorithms for approximate inference,” Ph.D. dissertation, University of Cambridge, May 2003.
- [30] T. Cover and J. Thomas, *Elements of Information Theory*, 2nd ed. Wiley Interscience, 2006.
- [31] G. Parisi, *Statistical field theory*. Perseus Books, 1988.
- [32] L. Christensen and J. Larsen, “On data and parameter estimation using the variational Bayesian EM-algorithm for block-fading frequency-selective MIMO channels,” in *Proc. IEEE International Conference on Acoustics, Speech and Signal Processing (ICASSP 2006)*, vol. 4, 2006, pp. 465–468.
- [33] B. Hu, I. Land, L. Rasmussen, R. Piton, and B. Fleury, “A divergence minimization approach to joint multiuser decoding for coded CDMA,” *IEEE J. Select. Areas Commun.*, vol. 26, no. 3, pp. 432–445, Apr. 2008.
- [34] C. N. Manchon, B. Fleury, G. Kirek, P. Mogensen, L. Deneire, T. Sorensen, and C. Rom, “Channel estimation based on divergence minimization for OFDM systems with co-channel interference,” in *Proc. IEEE International Conference on Communications (ICC’09)*, Jun. 2009.
- [35] C. N. Manchon, G. E. Kirek, B. H. Fleury, P. Mogensen, L. Deneire, T. B. Sorensen, and C. Rom, “Interference cancellation based on divergence minimization for MIMO-OFDM receivers,” in *Proc. IEEE Global Telecommunications Conference (GLOBECOM 2009)*, Dec. 2009, pp. 1–6.
- [36] D. Lin and T. Lim, “The variational inference approach to joint data detection and phase noise estimation in OFDM,” *IEEE Trans. Signal Processing*, vol. 55, no. 5, pp. 1862–1874, May 2007.
- [37] M. Nissilä, “Iterative receivers for digital communications via variational inference and estimation,” Ph.D. dissertation, University of Oulu, 2008.
- [38] X.-Y. Zhang, D.-G. Wang, and J.-B. Wei, “Joint symbol detection and channel estimation for MIMO-OFDM systems via the variational Bayesian EM algorithms,” in *Proc. IEEE Wireless Communications and Networking Conference (WCNC2008)*, Mar.-Apr. 2008, pp. 13–17.
- [39] J. Dauwels, “On variational message passing on factor graphs,” in *Proc. IEEE International Symposium on Information Theory (ISIT 2007)*, Jun. 2007, pp. 2546–2550.
- [40] G. Kirek, C. Manchon, L. Christensen, E. Riegler, and B. Fleury, “Variational message-passing for joint channel estimation and decoding in MIMO-OFDM,” in *Proc. IEEE Global Telecommunications Conference (GLOBECOM 2010)*, Dec. 2010, pp. 1–6.
- [41] E. Riegler, G. Kirek, C. Manchón, and B. Fleury, “Merging belief propagation and the mean field approximation: A free energy approach,” in *Proc. 6th International Symposium on Turbo Codes and Iterative Information Processing (ISTC 2010)*, Sep. 2010, pp. 256–260.
- [42] E. Riegler, G. E. Kirek, C. N. Manchón, and B. H. Fleury, “Merging belief propagation and the mean field approximation: A free energy approach.” [Online]. Available: arxiv.org
- [43] J. Tauge and C. Caldwell, “Expectations of useful complex Wishart forms,” *Multidimensional Systems and Signal Processing archive*, vol. 5, pp. 263–278, 1994.
- [44] 3GPP, “Base station (BS) radio transmission and reception,” 3GPP TS 36.104, V8.12.0 (2011-06) Technical Specification, 2011.